CHARACTERIZATION AND APPLICATION OF NEUTRON FLUX OF A 370 GBq ^{241}Am-Be IRRADIATING SYSTEM

BY

OLANDO ENOCH ANYENDA

A thesis

submitted for the partial fulfilment of the requirements for the award of Master of Science degree in Nuclear Science of the University of Nairobi.

Declaration

I declare that thesis is my original work and has not been submitted in any form for the award of a degree in any other University.

Signature..... Date 29/JUNE/2009

Olando Enoch Anyenda

This thesis has been submitted for examination with the approval of my University supervisors

Signature..... Date 29/6/2009

Mr. D. M. Maina

Director,

Institute of Nuclear Science and Technology,

University of Nairobi.

Signature..... Date 30/06/2009

Dr. A. O. Mustapha

Department of Physics,

University of Nairobi.

Abstract

Characterization of spatial neutron flux distribution above a 370 GBq ^{241}Am-Be neutron source in a moderating assembly has been performed experimentally. The source is surrounded by paraffin wax except for a cylindrical cavity along its axis, which also serves as the irradiation channel. This arrangement constitutes the so-called 'howitzer'. The experimental method was based on foil activation, using industrial grade Aluminum foils and analytical grades of Indium foil and Dysprosium Oxide (Dy_2O_3) pellet. The optimum flux positions for fast and thermal neutrons within the irradiation cavity were determined. The optimum thermal neutron fluxes lie between the distances 1.5 - 3.0 cm from the source. For bulk sample irradiation it is noted that meaningful thermal activation can also be achieved within the range of 0 - 6.0 cm from the source. The fast neutron flux decreases exponentially with distance from the source.

Some applications of the characterized irradiation facility were demonstrated; namely elemental analysis (for Si and Al concentrations) of geological specimens from Kanjera archaeological site, and the determination of hydrogen contents of some petroleum products in the Kenyan market. The determined Si and Al concentration were found to lie within the ranges 19.1± 9.9%

- 69.9± 26.6% and 18.0± 30.4% - 46.2± 73.9% respectively. On the other hand the hydrogen concentration in petroleum products was found to lie between 11.59± 0.36 – 13.90± 0.38 w%. This demonstrates important applications for which the characterized irradiation system could be useful. However, it must be stated that improvements have to be made inorder to minimize the large uncertainty as seen in the results.

Acknowledgements

I would like to thank my supervisors, Dr. A. O. Mustapha and Mr. D. M. Maina, for providing me with the necessary guidance and support that has seen the project come to a successful conclusion. I am especially indebted to them for their patience and encouragement even when I encountered some delays in the course of the project.

Also, I would like to acknowledge the help and support of the staff at the Institute of Nuclear Science and Technology in particular Mr. S. Bartilol and Mr. J. Njogu for their help during my lab work. I am greatly indebted to Dr. D. Braun, who gave me unlimited access to his geological specimens. Also, I am grateful to the management of National Museums of Kenya for the support they gave by allowing me to carry the samples from the museums.

Last but not least, my postgraduate studies could not have taken off had it not been to the generosity of the University's Board of Postgraduate studies to award me a scholarship. I, therefore unreservedly thank the Board for the generous provision.

Above all, I wish to thank any one who might have played a role towards the success of this project.

TO MY DEAR MUM VICTORIA ANYENDA, SISTER AND BROTHERS

Table of Contents

List of Tables

List of Figures

List of symbols and abbreviations

GBq	.....Gigabecquerels
cm	.....Centimeter
ml	.....Milliliter
IAEA	.....International Atomic Energy Agency
b	.....Barns
INDC	.....International Nuclear Data Committee
INS	.....Isotopic Neutron sources
eV	.....Electron volt
keV	.....Kilo electron volt
MeV	.....Mega electron volt
NAA	.....Neutron activation analysis
XRF	.....X-ray Fluorescence
ICP MS	.....Inductively coupled plasma mass spectroscopy
λ	.....Decay constant
f	.....Isotopic abundance of the isotope of interest
θ	.....Branching ratio of gamma-ray interest
ε	.....Detector efficiency
ϕ	.....Neutron flux
ρ	.....Density of Sample
η	.....Thermal Neutron Reflection Parameter
ω_i	.....Concentration of sample i

M .....Atomic mass number

N_A .....Avogadro's number

cps .....Counts per second

< .....Less than

> .....Greater than

n .....Neutron

p .....Proton

γ .....Gamma-ray

HPGe .....High purity Germanium

X .....Target nuclei

Y .....Product nuclei

Al .....Aluminium

Si .....Silicon

In .....Indium

TLD .....Thermoluminescent dosimeter

USGS .....United States Geological Survey

SRM .....Standard Reference Material

Dy_2O_3 .....Dysprosium oxide

INS .....Isotopic Neutron Source

Chapter 1

Introduction

1.1 Background

Neutrons are electrically neutral sub-atomic particles and therefore their interaction with atomic nuclei is of great significance. They are about 1840 times the masses of electrons, they possess magnetic dipole moment, and are quite unstable to beta decay with a mean life of about 10.6 minutes [Krane, 1988]. Generally, neutrons are classified according to their kinetic energies. They can be broadly divided into: slow/low energy neutrons with energies below 0.5 eV, intermediate neutrons with energies between 0.5 eV – 0.5 MeV and fast/high energy neutrons with energies above 0.5 MeV. The above classes can further be subdivided into more detailed categories as shown in the table below.

Table 1.1: Classes of neutrons [Dostal and Elson, 1980]

Type	Energy
Thermal	0.025eV
Epithermal	0.025 eV – 0.2 eV
Resonance	1 eV – 1000 eV
Intermediate	1 keV – 500 keV
Fast	> 0.5 MeV

When neutrons pass through matter they can either be scattered or captured by the nuclei in the matter giving rise to changes in energies of the particles involved or formation of new particles. Generally, all neutron interactions (except elastic collisions) produce secondary radiation such as gamma-rays, fast recoil protons and alpha particles.

Some of the intrinsic characteristics of neutrons have led to their widespread application as an indispensable tool for analyses and imaging of different forms of matter. Among the many applications of neutrons in elemental analyses are neutron activation analysis (NAA) and thermal neutron reflection method. NAA reveals the chemical properties (elemental composition) of a sample under investigation through absorptive nuclear reaction. The technique is widely applied in vast range of fields such as archaeology, geology, forensic science and semiconductor material manufacturing just to mention a few.

Thermal neutron reflection method depends on the concept of 'albedo' as explained by Amaldi and Fermi [1936]. Since its inception the method has been widely applied in the determination of hydrogen content of samples. It utilizes the large scattering cross section of hydrogen as compared with those of other elements. From

the measured induced intensity, the hydrogen content in the sample under investigation is determined using pre-calibrated curve constructed from standards of known hydrogen content [Jonah *et al*, 1999; Akaho *et al*, 2001].

There are a variety of sources of neutrons. Copious amounts of neutrons are usually produced in nuclear reactors and neutron generators (up to 10^{15} n/s). But modest fluxes are also produced by the so-called isotopic neutron sources (INS), e.g., ^{241}Am-Be, ^{252}Cf, etc. Isotopic neutron source are used in elemental analysis despite their modest output fluxes, which are of many orders magnitude lower than those of reactors and neutron generators. But even when the more prolific neutron sources (such as nuclear reactors) are available, Isotopic neutron source could still be sought after because they are relatively inexpensive for the low neutron emission (usually $< 10^{8}$ n/s) or due to their compact sizes, which facilitate some unique applications [Rapisarda and Samuelli, 1999; Kreft *et al*, 1989]. Isotopic neutron source such as Am-Be, have the advantage of producing relatively stable neutron fluxes over a long time, i.e., there is temporal stability of the neutron fluxes. Hence they are widely applied for calibration purposes in neutron dosimetry [Knoll, 1985; Nunes *et al*, 1997; Zevallos-Chaves and Zamboni, 2005].

Some of the disadvantages of INS, include their broad spectra (see Fig 1.1). Also, their neutron output cannot be pulsed, and it cannot be turned off, hence they have to be contained within bulky shielding at all times.

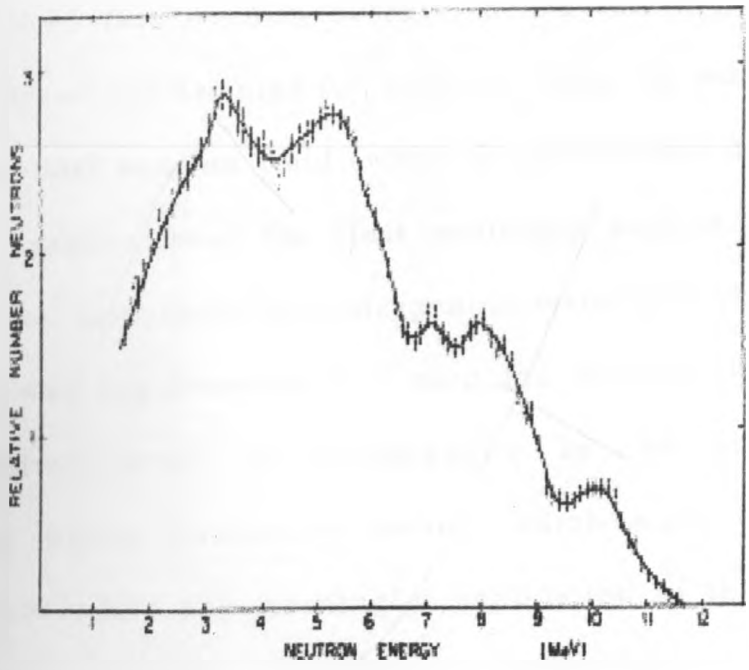

Fig 1.1 Neutron spectrum of Am-Be source [Adapted from IAEA, 1993].

The neutron field within the irradiation cavity of the howitzer has been characterized by determining the optimum irradiation position (i.e. optimum thermal and fast neutron fluxes) using the foil activation technique. Applications of the characterized ^{241}Am-Be based irradiation facility mainly in elemental analysis and

determination of hydrogen content in petroleum samples were carried out and presented in this thesis.

1.2 Statement of problem

Isotopic neutron sources have many unique applications, such as for elemental analyses as in NAA. But they suffer from modest (relatively low) fast neutron outputs, hence the requirement for large volumes of the samples for analysis. Also, in order to obtain enhanced thermal neutron field (which is particularly desirable for many NAA applications) the (fast neutrons) sources have to be moderated, i.e. surrounded by hydrogenous material such as paraffin wax. These two requirements (i.e. need for moderation and use of large samples) result in inhomogenity in the neutron field distribution within irradiation cavity, which must be carefully characterized before any meaningful application of the irradiation facility can be achieved. It is the goal of this study to characterize the 370 GBq Am-Be irradiating system based at the Institute of Nuclear Science and Technology (University of Nairobi, Kenya), so as to derive maximum benefits from its use in research and teaching.

1.3 Justification

There are some of the unique applications of isotopic neutron sources, e.g. elemental analysis of environmental, industrial and

biological materials. The neutron irradiation system at the Institute of Nuclear Science and Technology (University of Nairobi) consists of a 370 GBq ^{241}Am-Be neutron source installed in the cylindrical cavity/ bore inside a cylindrical block of paraffin wax of an outer dimension (50cm by 55cm). This geometrical arrangement is generally referred to as an 'howitzer'. The facility is yet to be fully utilized for routine irradiation. Following the successful characterization of this facility, it will compliment the existing XRF facility in the Institute for elemental analysis. NAA technique is notably a superior analytical technique compared to the XRF in number of ways. For instance, it is able to probe large volumes of material, it does not require elaborate sample preparations, it is non destructive (a requirement, e.g. for pricey or priceless archaeological artifacts), etc. These qualities of NAA will enhance the relevance of the institute, and expand the research capacities of the institute and hence that of the country as a whole.

1.4 Objectives

The overall objective of the study is to characterize the neutron field of the 370 GBq ^{241}Am/Be-based irradiator and set it up for applications in analysis of materials.

The specific objectives are to:

I. determine the axial thermal and fast neutron distributions in the irradiation cavity of the Am-Be irradiator.

II. determine the optimum positions of thermal and fast neutron irradiation of the irradiation facility.

III. determine the hydrogen content of some commercially available petroleum products in Kenya using the characterized facility.

IV. determine the Si and Al concentration in geological/ archaeological materials.

Chapter 2

Literature Review

2.0 Introduction

In this chapter brief historical perspective of neutron activation analysis (NAA) and thermal neutron reflection method is presented. Also a review of some of the applications of these techniques in providing solutions to analytical problems is presented.

2.1 Application of neutrons in analyses

The discovery of the neutron by James Chardwick in 1932 was followed by its applications as an invaluable investigating tool, e.g. in elemental analyses. The absorption of neutrons by nuclei provides a means of identifying and quantifying elements present in materials. Hevesy and Levi were credited for the first applications of NAA in the determination of the elemental concentrations in materials using isotopic neutron source [Glascock and Neff, 2003]. In the beginning of NAA, measurement of the induced activity was done using Geiger-Muller or proportional counters [Dybczyński, 2004]. The discrimination between various isotopes was based on the differences in half-lives and partly on the basis of the maximum energy of emitted beta rays (via appropriate absorbers).

The construction of intense neutron sources, introduction of high purity Germanium (HPGe) detectors coupled with improved data acquisition and data analysis instrumentations have transformed NAA into a very powerful analytical technique [Glascock *et al*, 2004]. NAA offers excellent sensitivity, great accuracy and precision. These explain its wide applications, e.g. in provenance studies of archaeological materials. The study involves tracing the origin of recovered materials (artifacts) with the aim of reconstructing their past history [Leach, 1997; Munita, 2004].

In carrying out the exercise Glascock and Neff [2003] traced the sources of obsidian artifacts from Chichen Itza using neutron activation analysis (NAA) with neutrons from a nuclear reactor. In another case study, sources of obsidian artifacts in central Mediterranean were successfully traced using the analysis of major elements in archaeological samples [Tykot, 2004]. These are but a few examples of elemental analysis of trace as well as major elements of geological and recovered materials. Elemental compositions of recovered ancient coins have also been carried out with neutron-based methods and NAA in particular. For example Kasztovszky [2004] and Win [2004b] analyzed Romanian silver denarii and ancient Myanmar coins non-destructively with NAA.

Apart from the neutron absorption reactions, the scattering interactions between neutrons and nuclei of materials can also provide information about the composition of materials. An example is the thermal neutron reflection technique which is based on the concept of 'albedo' [Mohapatra and Reddy, 2001]. The technique is based on neutron scattering. It was first developed by Buczko for determining bitumen content in asphalt concrete [see Jonah *et al*, 1997]. The technique takes advantage of the large scattering cross section of hydrogen as compared to the other elements. It is widely applied in determination of hydrogen content in solid and liquid materials.

The hydrogen content of a material could be a measure of the quality or authenticity of the material. For example a pure petroleum product will have different hydrogen concentration from its adulterated version. In a study carried out by Jonah *et al* [1999] the method was successfully applied to determine hydrogen content in some petroleum products in Nigeria. Similar studies have been carried out by Akaho *et al* [2001] for analyzing the Ghanaian petroleum products. In these studies they used neutrons from 185 GBq and 37 GBq Am-Be sources. The hydrogen content of the material under investigation is determined by placing a suitable thermal neutron probe between the sample and a fast neutron source.

As fast neutrons produced by the source undergo elastic collision they are thermalized. Some of the thermalized neutrons are back-scattered and detected by the probe. The measured intensity of the moderated neutrons is proportional to the hydrogen content in the sample. The technique has proved to be rapid and non-destructive since it requires minimum sample preparation [Akaho *et al*, 2002].

In order to successfully perform elemental analysis using neutrons, large quantities of neutrons are usually needed. This is because neutron flux has a direct proportionality to the sensitivity of the analysis. But the prolific neutron sources are expensive and usually beyond the budgetary capacity of most research institutions and universities [IAEA, 1988]. Therefore, in situations where the cost of neutron source is an issue, and/or for reasons of portability and certain degree of flexibility, isotopic neutron sources provide good alternatives [Knoll, 1985, Soete *et al*, 1972]. Some of the Isotopic sources, e.g. the ^{241}Am-Be, produce stable fluxes due to the long half-lives of the actinide element and this eliminates the problem of flux variability as in the case of reactors [Zamboni *et al*, 2001]. The intrinsic characteristics of isotopic neutron sources, make them suitable for applications such as explosive detection [Rapisarda and Samuelli, 1999] and for quality and on-line process control in industries [Garg and Batra, 1986; IAEA, 1999]. In geology, Idris *et*

al. [1998], Borsaru and Eilser [1981] and others [Das *et al*, 1989; Ambrosi *et al*, 2005] have also used isotopic neutron sources for field exploration of minerals as well as in provenance studies.

The preference for thermal neutrons in elemental analysis is because many nuclei have large nuclear reaction cross sections for thermal neutrons [Glasstone and Sesonke, 1994]. Thermal neutrons are obtained by moderating, that is slowing down fast neutrons, e.g. by surrounding the fast neutron source with suitable moderator, usually hydrogenous materials. A special geometrical arrangement of hydrogenous materials around a source, which is designed to concentrate thermalized neutrons in one direction is generally called the "howitzer" [Moses, 1964].

Several methods have been used for neutron detection [see Cember, 1985; Knoll, 1979]. Neutrons can be detected indirectly through nuclear reactions which produce charged particles such as protons, alpha particles, fission products as well as fast recoils. There are those based on nuclear reaction which emits prompt reaction products. Otherwise known as on-line detectors, they include the BF_3, ^3He detectors, fission chambers and others based on recoil-proton method. On the other hand, neutrons are also detected off-line, e.g. by foil activation method as used in the present study.

Chapter Three

Theoretical Principles

3.0 Introduction

Brief descriptions of production of neutron as well as principles of methods that employ neutrons are presented in this chapter.

3.1 Theory of neutron production in Am-Be Source

Owing to the unstable property of neutrons to beta decay and their quick absorption by the nuclei of surrounding materials, free neutrons do not exist for long in nature. Therefore neutrons have to be produced when required through suitable nuclear reactions. A typical nuclear reaction may be represented as:

$$X\ (x, y)\ Y$$

where

X – Target nuclei; x – Projectile; y – Recoil particle; Y – Product nuclei

In the production of neutrons, the projectiles can be protons, alpha-particles, deuterons, tritium, gamma radiation or heavy ions like lithium and beryllium. The reaction could be either naturally or artificially induced. In the case of INS, the reactions are induced by

projectiles from natural radioisotopes, e.g. alpha particles emitted from Americium.

Alpha particle (^{4}He) e.g., from Americium (^{241}Am) bombards beryllium (^{9}Be) and, upon radiative capture interaction, carbon (^{12}C) is formed as the product nuclei and neutron as a recoil particle [Mathew, 2002], i.e.

$$^{4}He + {}^{9}Be \longrightarrow {}^{12}C + n + 5.71MeV$$

A small self sufficient neutron source is formed by a mixture of Americium and Beryllium materials encapsulated in stainless steel.

3.2 Theory of neutron activation analysis (NAA)

NAA is a simple analytical method based on the use of the radioactivity induced in a material (when irradiated in a field of neutrons) to determine the chemical composition of the material. As neutron interacts with the target nucleus, a compound nucleus is formed which is in excited state. The compound nucleus (radioactive nucleus) decays with emission of radiation. The induced activity can be measured using standard methods for quantitative and qualitative analysis of the sample.

Suppose a sample containing N target (non-radioactive) nuclei is exposed to a flux ϕ ($ncm^{-2}s^{-1}$) of neutrons. The number (N_0) of

radioactive nuclei formed after time (t) directly depends on N and ϕ, i.e.:

$$N_0 \alpha N \phi \quad \ldots\ldots 1$$

or

$$N' = N\sigma\phi \quad \ldots\ldots 2$$

where α is the proportionality sign and σ (in barns or 10^{-24} cm^2) is the proportionality constant, i.e. the probability of the nuclear reaction taking place.

Since the product radionuclide begins to decay immediately it is formed, the exponential decay law must be obeyed, so that $N'(t)$ is given by:

$$N'(t) = N\sigma\phi e^{-\lambda t} \quad \ldots\ldots 3$$

where λ is the decay constant of the created radionuclide given by $0.693/t_{1/2}$ and $t_{1/2}$ is the half life. It must be pointed out, however, that both σ and ϕ depend on the energy of neutron (see appendix 2) . N can also be expressed as:

$$N = \frac{m N_A f}{M}$$

where m is the mass of the irradiated element of interest, N_A is the Avogadro's number, M is the atomic mass of element and f is the isotopic abundance of the isotope of interest.

This then means that the integration of equation 3 over the time range, t=0 and $t = t_i$ gives the total number of radioactive nuclei present at the end irradiation, i.e.

$$N(t_i) = \int_{t=0}^{t_i} \frac{m N_A \sigma \phi e^{-\lambda t} f}{M} dt$$

$$= \frac{m N_A \sigma \phi}{M \lambda} f\left(1 - e^{-\lambda t_i}\right) \ldots\ldots\ldots\ldots\ldots\ldots\ldots\ldots 4$$

where

t_i - irradiation time

$\left(1 - e^{-\lambda t_i}\right)$ - saturation factor that accounts for decay during irradiation

In the event that irradiation and counting are not done simultaneously, i.e. the counting of induced activity commences after a decay period of time t_d. (the time period between the end of

irradiation and start of counting), then number $N(t_d)$ of radioactive nuclei at the beginning of counting is given in terms of the number ($N(t_i)$) at the end of irradiation as follows:

$$N(t_d) = N(t_i)e^{-\lambda t_d}$$

or

$$= \frac{mN_A\sigma\phi}{M\lambda} f\left(1 - e^{-\lambda t_i}\right)\left(e^{-\lambda t_d}\right) \ldots\ldots\ldots\ldots\ldots\ldots\ldots 5$$

After counting period of time t_c, the number of radioactive nuclei that decay will be given by the difference between the numbers at the beginning and end of the counting. This number is mathematically expressed as:

$$N(t_c) = N(t_d)\left(1 - e^{-\lambda t_c}\right)$$

or

$$N(t_c) = \frac{mN_A\sigma\phi}{M\lambda} f\left(1 - e^{-\lambda t_i}\right)\left(e^{-\lambda t_d}\right)\left(1 - e^{\lambda t_c}\right) \ldots\ldots\ldots\ldots 6$$

Therefore the activity of the material within the counting period is

$$A(t_c) = N(t_c)\lambda = \frac{mN_A\sigma\phi}{M} f\left(1 - e^{-\lambda t_i}\right)\left(e^{-\lambda t_d}\right)\left(1 - e^{-\lambda t_c}\right) \ldots 7$$

For a sample of given mass m_s containing m of the irradiated element, the concentration (ω) of the element is:

$$\omega = m/m_s \quad \ldots\ldots\ldots\ldots\ldots\ldots\ldots\ldots\ldots\ldots\ldots\ldots\ldots\ldots\ldots\ldots 8$$

Equation 7 can then be rewritten as:

$$A(t_c) = \frac{m_s\, \omega N_A \sigma \phi}{M} f\left(1-e^{-\lambda t_i}\right)\left(e^{-\lambda t_d}\right)\left(1-e^{-\lambda t_c}\right) \ldots\ldots\ldots 9$$

However, the detection system does not detect all these decays. For example, the number of gamma rays counted by the gamma-ray detector of the spectrometric system is only a small percentage of the number of decays. These discrepancies are usually associated with the detector efficiency and the branching ratio of the gamma-line. After correction has been made for these sources of error, the yield (Y) or count rate registered by the detecting system during counting time will be given by:

$$Y(t_c) = \varepsilon \theta A(t_c) \ldots\ldots\ldots\ldots\ldots\ldots\ldots\ldots\ldots\ldots\ldots\ldots\ldots\ldots 10$$

where

ε - detector efficiency

θ – branching ratio of gamma-ray of interest

Therefore, if all other variables are kept constant the detector response or yield will be a direct measure of the elemental concentration in a sample of given mass. The above process is known as delayed gamma neutron activation analysis (DGNAA). On other hand, if the measurement of gamma rays is done during irradiation the process is known as prompt gamma neutron activation analysis (PGNAA) and the detector response may be expressed as [Sudarshan *et al*, 2001]

$$N = \frac{\varepsilon \phi \sigma T m N_A f \theta}{M} \quad \ldots\ldots\ldots\ldots\ldots\ldots\ldots\ldots\ldots\ldots\ldots\ldots 11$$

where T is the total time for the irradiation and all other terms remain as previously defined.

3.3 Theory of Thermal Neutron Reflection Method

The basis of thermal neutron reflection method is the measurement of thermal neutron reflection parameter due to the scattering of neutrons as they interact with hydrogen-containing samples. The reflection parameter is directly proportional to hydrogen content present in the sample. The technique utilizes the large scattering cross section of hydrogen as compared to the other elements. As fast neutrons from the source interact with the hydrogenous sample, they

undergo continuous collisions until they become thermalized. An appropriate thermal neutron probe is usually placed between the fast neutron source and the sample. Some of the thermalized neutrons are scattered in the direction of the probe and get detected. The measured induced intensity in the probe allows for the hydrogen content to be determined using a pre-calibrated curve.

Assume that I is the induced count rate measured in the probe after reflection of thermalized neutrons with the presence of sample (cps) whose density is ρ (gcm^{-3}) while I_0 is without. Such that the excess count rate which gives the reflection parameter (η) is mathematically expressed as [Akaho *et al*, 2002]:

$$\eta = \frac{I - I_0}{\rho I_0} \quad \ldots\ldots\ldots\ldots\ldots\ldots\ldots\ldots\ldots\ldots\ldots\ldots\ldots\ldots 12$$

η has the units inverse that of density ($cm^{-3}g$).

Chapter Four

Materials and Methods

4.0 Introduction

In this chapter description of materials applied in this study is made. The procedures used in the analyses of geological materials and petroleum products are also presented.

4.1 Materials

The materials used in this study include the following: the Am-Be irradiating system, activation foils, standards, samples, samples holders as well as the gamma ray spectrometer.

4.1.1 The Am-Be irradiating system

The irradiating system (Figure 4.1.) consists of a 370 GBq ^{241}Am-Be neutron source. It is cylindrical capsule of 3.0cm diameter and 5.0cm overall length. The neutron emission rate is 2.2×10^{7} ns^{-1} ± 10%. The fast neutrons from the source are moderated (slowed down) by its nearly 4π immersion within a volume of paraffin wax. An axial cylindrical cavity (3.2cm diameter by 23.5 cm height) bored through the solid paraffin block (50cm diameter by 55cm height) makes the system behave like an howitzer (Moses, 1964).

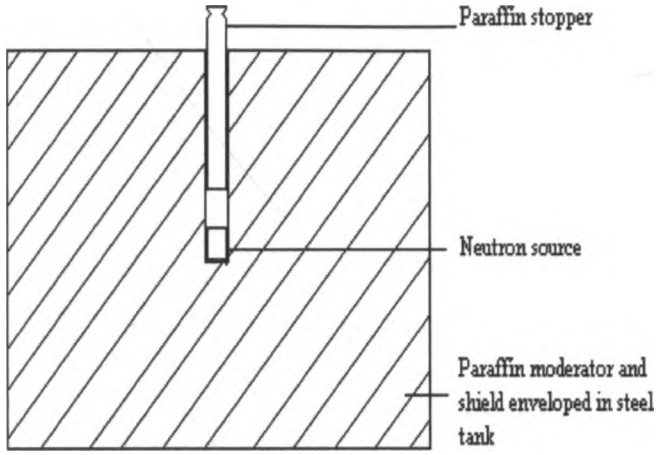

Fig 4.1 Neutron irradiation facility.

4.1.2 Activation foils for neutron detection

One of the major components of the study is an investigation of the neutron flux distribution within the irradiating cavity.

Figure 4.2 The flux monitors; the three on lowest row are In foils, on top of them are 3 Al foils and topmost is a pellet of Dy_2O_3.

This was carried out using activation foils, comprising industrial grade aluminium foils (3cm diameter by 0.3cm thickness), and analytical grades of indium foil and dysprosium oxide (Dy_2O_3) pellet (Figure 4.2). Circular perspex discs (3 cm diameter and variable thickness) were used to vary the distance between the source and the foils during the flux monitoring procedure.

4.1.3 Standards, samples and sample holders

The standards or reference materials used in the study included; pulverized Rhyolite (RGM-1), Andesite (AVG-2), and Granodiorite (GSP-2) from United States Geological Survey (USGS) [USGS, 2007] as well as analytical grade silicon dioxide (SiO_2) from Adrich chemical company Inc.

The samples analyzed for elemental concentrations were pulverized archaeological/geological materials collected from Kanjera archaeological site of South Nyanza in Kenya (Braun, 2006). The geological samples and standards were irradiated in plastic vials (2.7cm diameter by 3.5 cm length).

Analytical grades of liquid hydrocarbons; acetic acid (CH_3COOH), benzene (C_6H_6), iso-butyl methyl ketone ($(CH_3)_2CHCH_2COCH_3$) and ethanol (C_2H_5OH), water (H_2O), as well as petroleum products were

also analyzed to determine their hydrogen contents. These samples were held in 250 ml plastic beakers of dimension (6.8cm diameter by 9.4 cm height) during the analysis.

Fig. 4.3 Sample holders for pulverized geological and petroleum materials.

Fig 4.4 Standards used for activation analysis of geological materials.

4.1.4 The gamma-ray spectrometer

The induced radioactivity in samples/neutron-monitors was measured using a gamma-ray spectrometer. It consisted of HPGe gamma-ray detector, pre-amplifier, linear amplifier, multi-channel analyzer (MCA), personal computer (PC) and printer. Figure 4.5 shows the block diagram of the gamma spectrometer and Figure 4.6 is a photograph of lead shield housing the detector assembly as well as the other electronics for spectral data processing.

The detector is a coaxial (5.74 X 5.79cm) HPGe with 30% efficiency relative to the 3" x 3" NaI (Tl) detector. Its original resolution was 1.8 keV (FWHM) at 1.33 MeV peak of Co-60. However, its resolution at the time of these measurements was about 4 keV. The MCA used is a PC based card supplied with appropriate software personal computer analyzer (PCA3) for data acquisition and analysis. Further data analyses were also performed with the MS Excel.

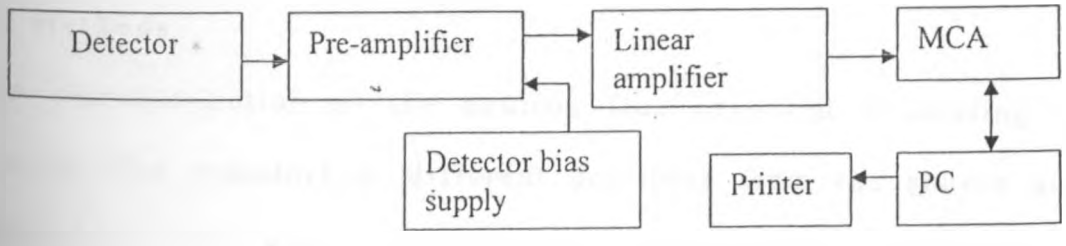

Fig 4.5 Block diagram of the HPGe detector-based gamma-ray

spectrometer.

Fig 4.6 The gamma-ray spectrometer setup comprising the HPGe detector (inside the lead shield) and the associated electronics.

The samples/monitors were lowered into - and removed from – the irradiation channel using polyethylene strings. Activated samples are also held in lead box prior to – and after – gamma-ray analysis.

4.2 Methods

The characterization of the neutron flux involved irradiating of neutron flux monitors at different positions from the source and determining the induced intensity and consequently the elemental concentration from equation 9 (chapter 3). The procedures used in this study are described in the following sections for analysis of

geological materials for elemental content and determination of hydrogen content in petroleum products.

4.2.1 Characterization of the neutron flux

i) Foil Activation

The axial neutron flux distribution in the cylindrical cavity above the source was investigated by varying the distance of the moderating perspex between the source and the monitor(s). For the Al foil, the procedure involved 20 minutes of irradiation followed by 10 minutes of counting. The same procedure was repeated at different positions from the source. In order to make corrections for different times of cooling, the time between the end of irradiation and start of counting was noted. This was necessary as the irradiation and counting apparatus were located in two adjacent laboratories.

For the case of indium foil, 3 hour irradiation was performed followed by 10 minutes counting. Three (3) hours of irradiation and 30 minutes of counting was also used in the case of dysprosium oxide pellet. In all cases, the cooling time was noted. The position of the source was maintained through out the irradiation exercise.

ii) Measurement of induced activity by gamma-ray spectrometer

The induced activities were measured using the gamma-ray spectrometer setup described in section 4.1.3. The gamma-ray spectrometer was calibrated (for energy) using a multi-nuclide standard material (SRM -1). The peaks used were those of ^{241}Am, ^{137}Cs and ^{60}Co, i.e. 59.54 keV, 661.66 keV, 1173.24 and 1332.5 keV respectively.

For the Al foil, the peaks of interest are 844 keV of ^{27}Mg from the nuclear reaction ^{27}Al (n, p) ^{27}Mg and 1779 keV of ^{28}Al from the nuclear reaction ^{27}Al (n, γ) ^{28}Al. The other gamma lines used were 1293 keV of ^{116}In from the reaction ^{115}In (n, γ) ^{116}In for In-foil and 95 keV of ^{165}Dy from the reaction ^{164}Dy (n, γ) ^{165}Dy for the Dy_2O_3 pellet.

Inorder to ensure reproducible counting geometry, a jig was constructed that hold both the sample and the detector firmly together during counting. The axial neutron distribution within the howitzer was determined using the conventional NAA equation (equ. 7). Since the neutron foil monitors were made from the same sheet/wire, only the time and/or mass of monitor corrections were made while the other parameters were reduced to unity. To

normalize the data for different source distances, the ratios of relative neutron fluxes were computed by dividing all through by the highest flux value. Plots of relative neutron flux versus distance from the source were made giving the flux profile within the irradiating cavity.

4.2.2 Application of INS methods in analysis of geological materials

Pulverized archaeological rock samples from the Kanjera archaeological site in Southwestern Kenya were analyzed based on comparative method using the USGS reference materials (AGV-2, RGM-1, and GSP-2) as well as silicon dioxide (SiO_2) standard. The method involves comparison of the induced intensities for both standard and unknown samples. Assuming no temporal variation of fluxes occurs (this is so for long-lived neutron sources like Am-Be) the standards and unknown samples will experience the same neutron fluxes if the same irradiation geometry is maintained. Both unknown samples and the standards were irradiated in identical (reproducible) irradiation and counting conditions. They were placed in identical plastic vials such their masses were about 15.46 g. All irradiations were carried out at the optima flux positions identified during the characterization experiment. For optimum thermal neutron activation, each sample/standard was irradiated for

30 minutes at 0.4 cm distance from the source. Reproducibility was also enhanced by irradiating similar quantities of samples in similar sample holders.

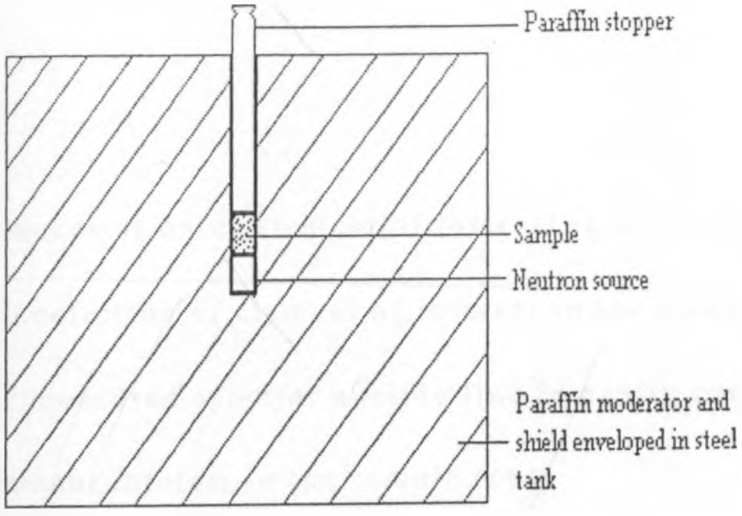

Fig 4.7 Experimental set-up for elemental determination of geological materials.

The calibrated (for energy) gamma-ray spectrometer is used to quantify the elemental concentrations in the unknown sample. This involves a measurement of the background activity of the samples before they were irradiated in the beam of neutrons. The induced intensities were also counted after irradiation.

The elemental concentration in a sample is obtained by solving the equation [Win, 2004a]:

$$\omega_{sam} = \frac{\omega_{std} I_{sam}}{I_{std}} \quad \ldots\ldots\ldots\ldots\ldots\ldots\ldots\ldots\ldots\ldots\ldots\ldots\ldots\ldots 13$$

where

ω_{sam} - is concentration of element of interest in the sample (%)

ω_{std} - is concentration of element of interest in the standard (%)

I_{sam} - is the measured spectral nuclide line intensity corresponding to element interest in the sample (cps)

I_{std} - is the measured spectral nuclide line intensity corresponding to the element interest in the standard (cps)

Both I_{sam} and I_{std} were corrected for background contributions.

4.2.3 Determination of hydrogen content of Petroleum products

The experimental set-up used in the study is shown in Fig 4.8. The sample is placed right at the top of the cavity so that it experiences a beam of fast neutrons directly from the source. A layer of boric acid covers the top of the howitzer. The sample holder (250 ml cylindrical plastic beakers) with a thermal neutron probe (In-foil)

fastened to its bottom, was positioned such that the indium is along the axis of the cavity in a reproducible geometry. The indium detector registers the amount of thermal neutrons backscattered from the sample, as a measure of the hydrogen content of the sample.

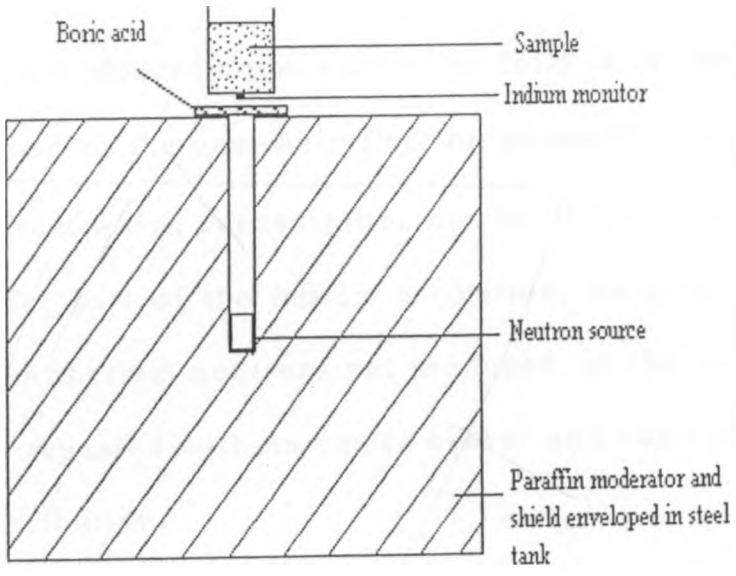

Fig. 4.8 Experimental set-up for the determination of hydrogen content of petroleum products.

The irradiation was carried out for one hour followed by the measurement of the induced intensity in the In-foils for 30 min after a cooling time of 20 min.

In the experimental set-up, the layer of boric acid between the fast neutron source and the sample is to enhance signal to background

(noise) ratio by ensuring that only the contributions of thermalized neutrons coming from the sample are recorded. Cadmium foils are commonly used for this purpose, but in the absence of cadmium foil, boric acid was used since it contains boron which also has high absorption cross section for thermal neutrons [Kreft *et al*, 1989].

The relative excess induced count rate in the foils in the presence of a sample is related to the neutron reflection parameter (η) as given in equation 12 from which concentration can be determined. In order to compensate for part of the indium activation, which might have resulted from the thermal neutrons not produced in the sample, the experiment was repeated with an empty beaker and corrected as the background contribution.

Chapter Five

Results and Discussions

5.0 Introduction

In this chapter the results of measurements for the neutron (both relative thermal and fast) flux distributions within the irradiation cavity of the howitzer based on foil activation are presented. Also presented are results of elemental concentrations of Al and Si in geological samples and the hydrogen content in petroleum products that were analyzed.

5.1 Characterization of axial variation of neutron fluxes in the cavity

Both In and Dy are known for their high thermal neutron cross-sections (160 b for In and over 800 b for Dy) according to Gubbi [2004]. This is why they were chosen for the determination of the spatial variation of the thermal neutron flux. On the other hand, Al has a moderate thermal neutron flux cross-section (0.23 b) but it also has a moderate cross section for fast neutrons. Therefore Al can be used to monitor both fast and thermal neutrons simultaneously.

Figures 5.1, 5.2, 5.3 and 5.4 show the variation of neutron fluxes with distance from the neutron source. The curves reveal that

optimum thermal neutron fluxes are obtainable within the range of 0 - 6.0 cm, 0 - 5.5 cm and 0 - 3.0 cm distances from the source for In, Dy and Al foils respectively. In all cases, the moderation of the fast neutrons reached the maximum near to the source (approximately 2.5 cm for In and Dy_2O_3, and 1.5 cm for Al). This can be attributed to the fact that the scattering cross section of hydrogen increases rapidly with decrease in neutron energy.

Table 5.1 Data for relative thermal neutron flux as measured by In-wire at various distance from the source.

Distance from the source (cm)	*Relative thermal flux values	Relative error (%)
0.0	0.6	2.6
0.4	0.8	2.5
0.8	0.7	2.6
1.2	0.8	2.5
1.6	0.8	2.6
2.0	1.0	2.4
2.4	0.9	2.5
2.8	0.9	2.4
3.2	0.9	2.4
4.0	0.8	2.5
5.0	0.7	2.6
7.0	0.5	2.8
10.0	0.3	3.4
13.7	0.1	4.0

*Relative thermal flux = flux at distance x / maximum flux

Thus if a neutron from the source collides with atoms in the moderating medium and experiences a large energy loss, the cross section for additional collision is large. Hence, the probability of moderating the produced neutrons is large near the position of first collision. Subsequently, after the maxima points were reached, the thermal neutron fluxes sharply decreased in the case of In and Dy while slightly less sharp for Al foils. These results agree with the results obtained in earlier study by Mustapha [1992].

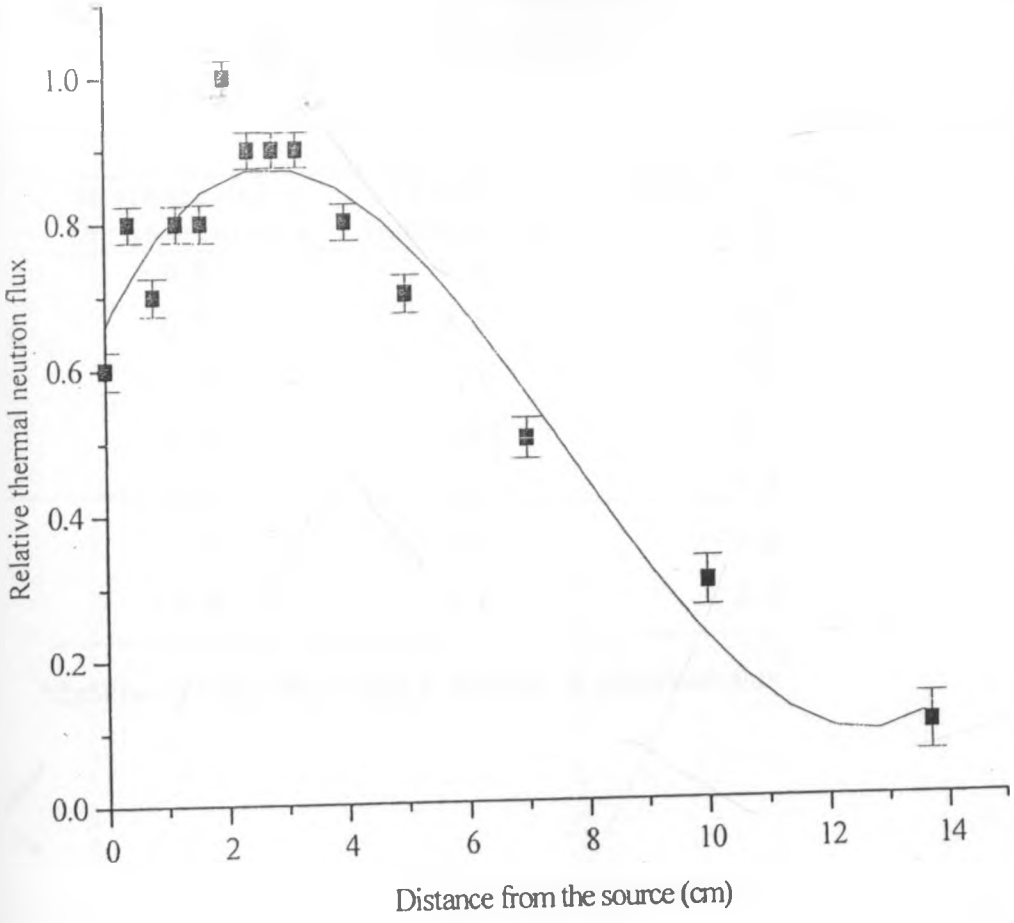

Fig 5.1 Graph of relative thermal neutron flux as a function of distance from the source as determined by In-wire probe.

Table 5.2 Data for the relative thermal neutron flux as measured by Dy_2O_3 pellet at varying distances from the source.

Distance from the source(cm)	*Relative thermal flux	Relative Error (%)
0.0	0.6	1.5
0.4	0.5	2.5
1.0	1.0	1.4
2.0	0.9	1.4
2.4	0.8	1.8
7.0	0.4	1.8
10.0	0.2	2.3

*Relative thermal flux = flux at distance x/ maximum flux

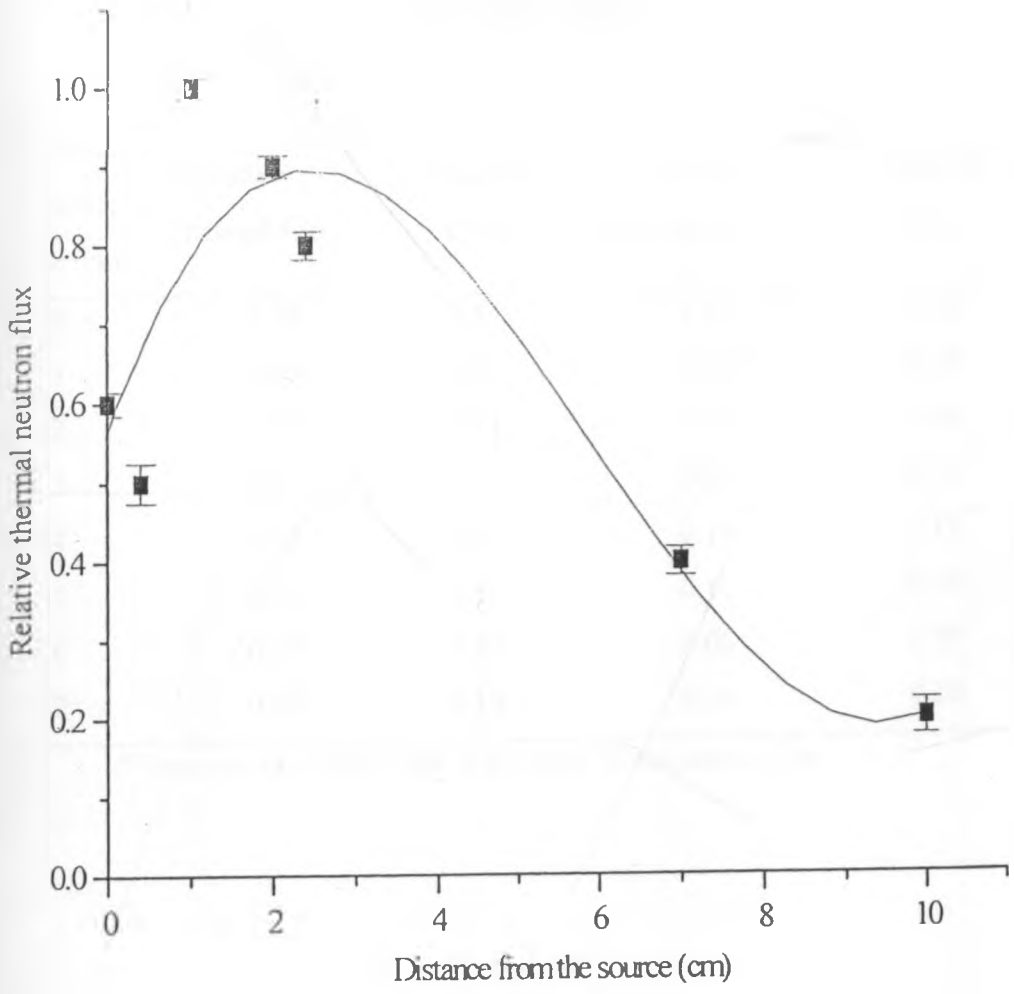

Fig 5.2 Graph of relative thermal neutron flux values as determined by Dy_2O_3 pellet at varying distances from the source.

Table 5.3 Data for the relative neutron flux as measured by Al foil at various distances from the source.

Distance from the source (cm)	*Relative Thermal flux	Relative error	**Relative fast neutron flux	Relative error
0	0.70	0.14	1.00	0.08
1	1.00	0.12	0.62	0.08
2	0.77	0.11	0.36	0.10
3	0.81	0.13	0.23	0.12
4	0.44	0.25	0.15	0.15
5	0.51	0.15	0.10	0.14
6	0.29	0.29	0.06	0.19
7	0.31	0.19	0.04	0.20

**Relative fast flux = flux at distance x/ maximum flux

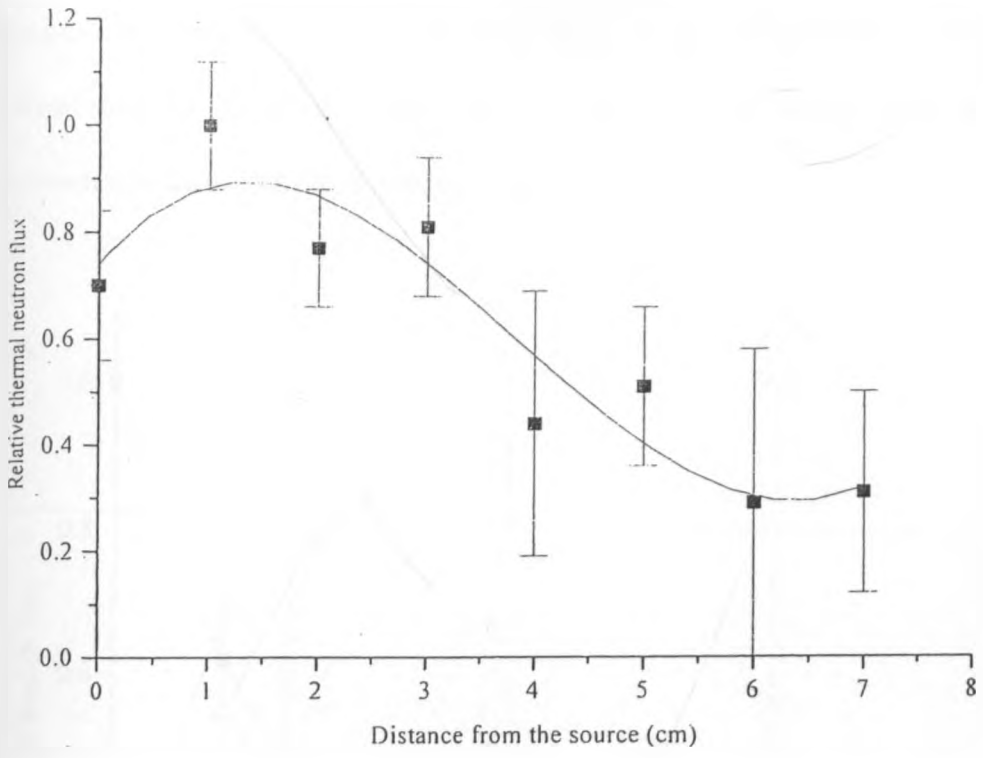

Fig 5.3 Graph of relative thermal neutron flux as a function of distance from the source as determined by the Al-foil monitor.

In the case of fast neutrons curve, it sharply decreases with increase in the distance between source and Al probe. However, one could still detect appreciable but slowly varying fast neutrons at distances far away from the source (see Fig. 5.3). This may be due to neutron hardening. Since the neutron scattering cross section for hydrogen decreases with increase in neutron energy, the more energetic neutrons in the primary spectrum are the less attenuated. Hence, with the increase distance from the source, the percentage of these

energetic neutrons become more and more. This means that at large distances from the source, neutron flux is predominantly composed of neutrons that have made no collision or at most a few angle collisions producing less energy loss.

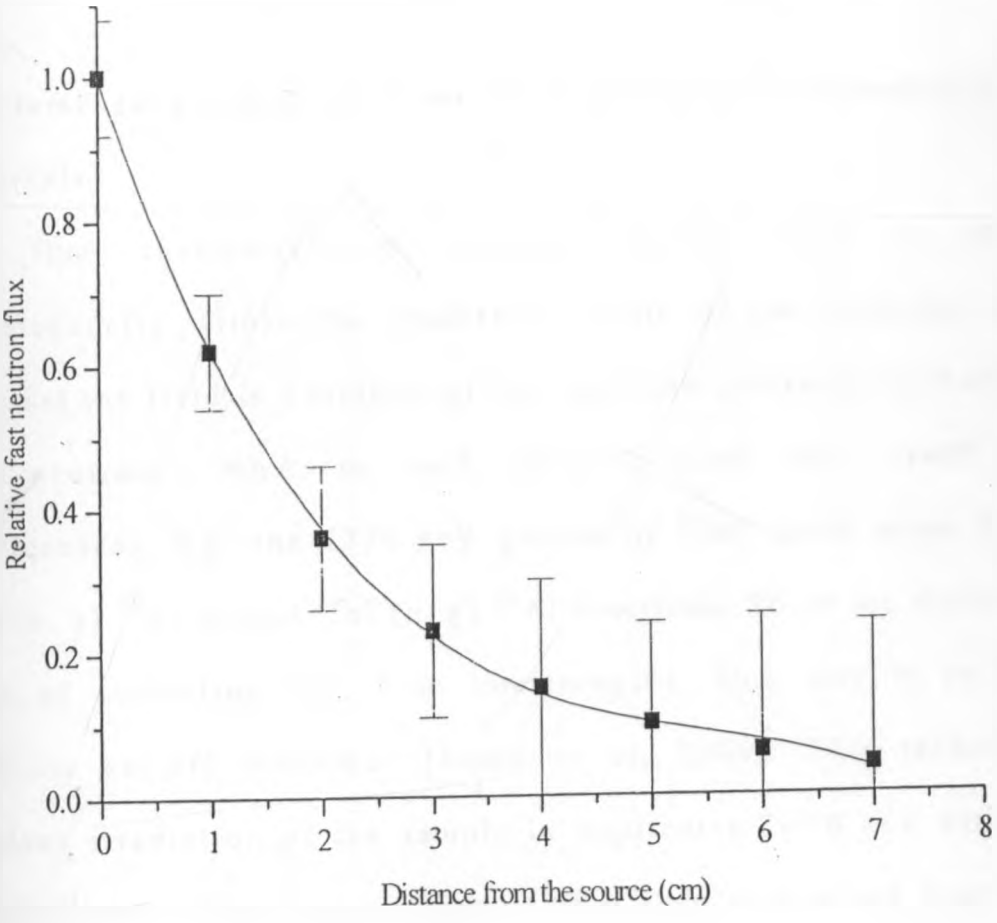

Fig 5.4 Graph of relative fast neutron flux as a function of distance from the source.

Whilst the general trend of both neutron fluxes seems to in agreement with theory, the fast neutron curve continued to decrease

appreciably even at large distance from the source. This could partly be due to the grade of Al foil used and installation of the source in nearly 4π in paraffin wax as well as the presence of paraffin stopper that was always placed on top of the monitor during irradiation.

5.2 Elemental analysis of Si and Al in geological/archaeological materials

The flux characterization exercise showed there is steep inhomogeneity within the irradiation cavity of the howitzer, and also that the field is a mixture of fast and slow (thermal, epithermal etc) neutrons. NAA in such neutron field may result in interferences, e.g. the 1779 keV gamma of ^{28}Al could result from ^{27}Al (n, γ) ^{28}Al or/and ^{28}Si (n, p) ^{28}Al reactions. There are different ways of correcting for these interferences. One way is to use cadmium cut-off technique [Jonah *et al*, 2004]. This technique involves irradiation of the sample in duplicates (with and without cadmium foil). The concentration of Si is then determined from the measured count rate from activities induced in the sample covered with Cd foil during irradiation using 1779 keV gamma line due to ^{28}Si (n, p) ^{28}Al reaction. The Al concentration is determined from the difference between the count rates under 1779 keV gamma-line for the uncovered and that of covered samples.

Alternatively the 1273 keV gamma line of ^{29}Al can be used to determine silicon accurately. This gamma-line from ^{29}Si (n. p) ^{29}Al reaction, is usually free from interferences [Koch, 1960]. The contribution of Si in the 1779 keV is then used as a correction to determine the Al concentration. This method was adapted in the present study to determine the elemental concentration of both Silicon and Aluminium in geological materials (details for the procedure is described in appendix 2). Table 5.4 and 5.5 shows the result of elemental concentrations of Al and Si in reference standards and some unknown geological samples respectively.

Table 5.4 Concentrations of Si and Al in reference standards [Adrich Chemical Com. and USGS, 2007].

Sample code	Si conc. (%)		Al conc. (%)	
	Reference	Obtained in this study	Reference	Obtained in this study
SiO_2	46.66	-	-	-
AGV-2	27.7 ± 0.35	19.1 ± 9.9	8.95 ±0.11	8.99 ± 15.9
RGM-1	34.3 ± 0.25	44.5 ± 18.7	7.25 ±0.10	7.31 ± 11.5
GSP-2	31.1 ± 0.40	31.7 ± 14.6	7.88 ±0.11	7.88 ± 12.5

Table 5.5 Concentrations of Si and Al in some geological samples from Kanjera archaeological site.

Sample code	Obtained Si conc. (%)	Obtained Al conc. (%)
LAW 1	42.4 ± 18.2	18.6 ± 29.2
MAKA 20; 9-28-02	46.6 ± 19.6	ND
MKY-2	69.9 ± 26.6	ND
MAKA 01;9-27-02	31.8 ± 14.6	46.2 ±73.9
MANG 01;10-11-01	53.0 ± 21.7	ND
NGEG Φ2;9-30-01	31.8 ± 14.6	ND
MANY Φ2; 9-19-01	10.6 ± 6.5	45.2 ± 80.2
NYASA;10-11-01	46.6 ± 19.6	ND
OJAWΦS; 9- 24 -02	19.1 ± 9.9	18.0 ± 30.4

ND – not detected or below detection limit

The detection limits for Silicon and Aluminium concentration for this experimental set-up are 0.05% and 0.01% respectively (details in Appendix 2).

The uncertainties associated with the elemental concentrations of Al and Si in geological samples by NAA are normally high. For example Schweitzer *et al* [1985] showed that in determining Al concentration after correction for Si contribution based on ^{29}Si (n, p) ^{29}Al delayed activity, an error of upto ±100% could be obtained. In this study the error in the Si concentration ranges from ±38% - ±61% while an error of over 150% is obtained in Al concentration.

The uncertainty in determining Al are particularly high because it incorporates (see Table 5.5) peak area errors of both the 1273 keV (of Si) and 1779 keV (of Si and Al). Any uncertainty in determining the Si concentration further increases the uncertainty and decrease the accuracy of Al measurement.

Another possible contributing factor to the peak area error is the cooling time. Due to the short half life of ^{28}Al (2.23 min) the cooling time should be as short as possible to obtain well resolved peak. The limit of detection for Al and Si with this procedure can be enhanced (reduced) by optimizing the cooling time, as well as by minimizing the uncertainties in the peak area estimation.

5.3 Determination of hydrogen content in petroleum products

Here discussion of the results of the two steps, i.e. preparation of a calibration curve using known standards and its application in determining the hydrogen content in unknown samples is made.

i) Hydrogen content of standards materials (for Calibration)

The calibration curve (Figure 5.5) of the reflection parameter versus hydrogen content was prepared using standards of known hydrogen content (see Table 5.6). It is clearly noted that the reflection parameter (η) is directly proportional the hydrogen content of the

samples. The higher the hydrogen content the higher the value of the reflection parameter for any given sample. On the contrary, (η) correlates negatively with concentrations of carbon and oxygen as shown by the plot of η vs. (O + C)/ H (Fig.5.6). Therefore the reflection parameter is a measure of the hydrogen content of materials.

Table 5.6 Data on standards used to construct the calibration graph.

Sample	Density (gcm^{-3})	Hydrogen conc. (w %)	Reflection parameter η ($cm^{-3}g$)	Weight ratio (O+C)/ H
Acetic acid (CH_3COOH)	1.048	6.67	0.909 ±0.41	14.00
Benzene (C_6H_6)	0.878	7.69	1.726 ±0.40	12.00
Water (H_2O)	1.000	11.11	2.067 ±0.36	8.00
Iso-butyl methyl ketone $(CH_3)_2CHCH_2COCH_3$	0.799	12.00	2.414 ±0.35	7.33
Ethanol (C_2H_5OH)	0.790	13.04	2.863 ±0.36	6.67

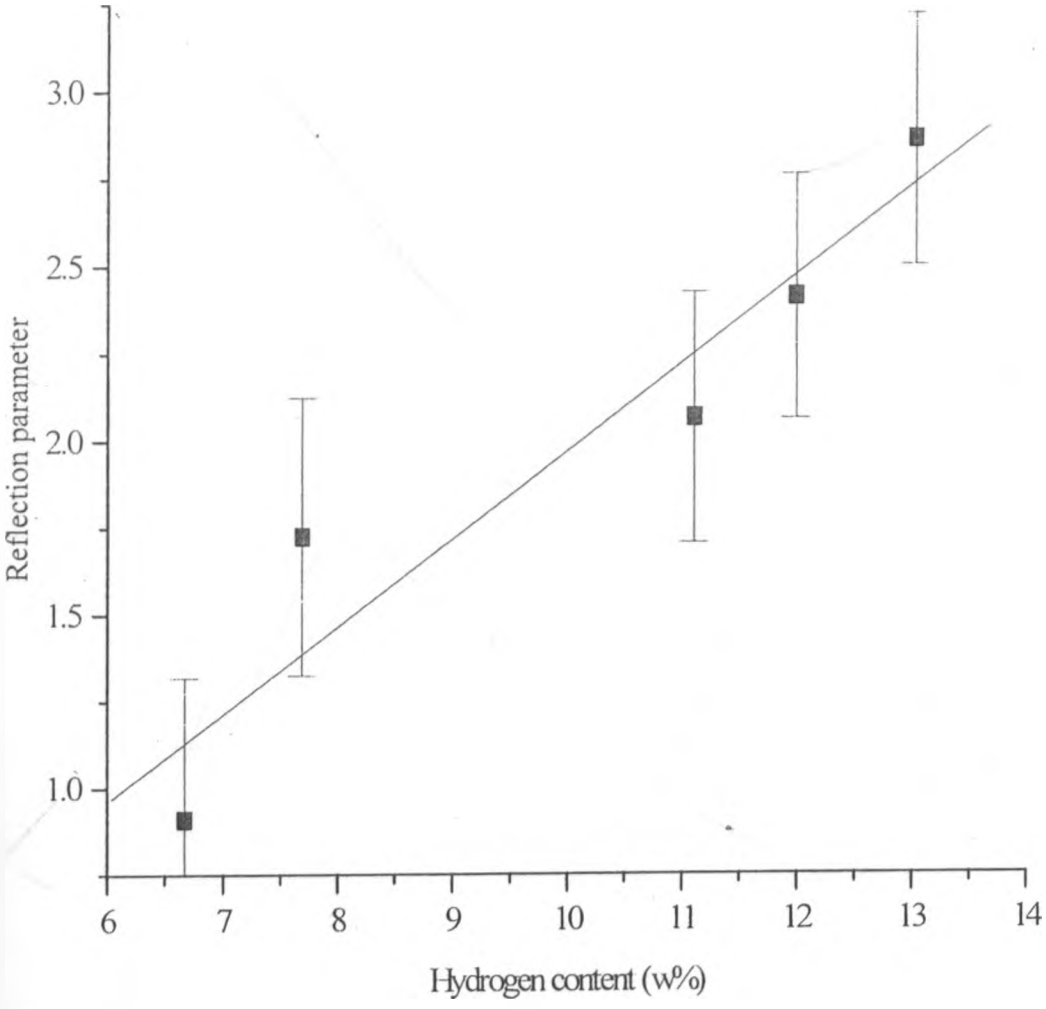

Fig 5.5 Calibration curve for the determination of total hydrogen content in petroleum products.

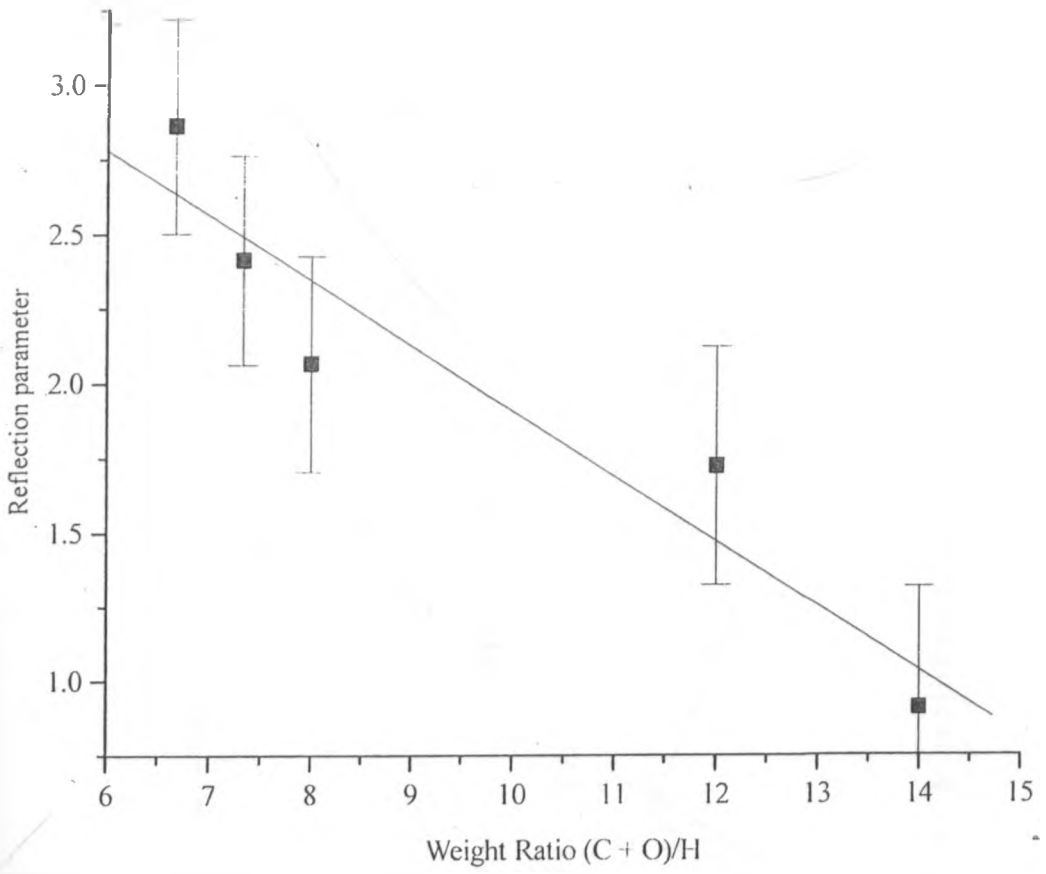

Fig 5.6 Plot representing the reflection parameter as a function of weight ratio(C+O)/H.

ii) Determination of Hydrogen content of Petroleum products

Using the calibration curve(Fig. 5.5) the hydrogen content of some of the petroleum products commercially available in Kenya were determined. As shown on table 5.7, the value range from 11.59±0.36 w% (for diesel) to 13.90±0.38 w% (for lubricating oil).

Table 5.7 Results of Hydrogen content in petroleum products

Petroleum Products	Density ($g\ cm^{-3}$)			Hydrogen content (w %)		
	Ref 1	Ref 2	This work	Ref 1	Ref 2	This work
Petrol	0.744	0.744	0.754	12.30 ± 0.15	12.54 ± 0.15	12.18 ± 0.36
Diesel	-	0.887	0.858	-	12.75 ± 0.17	11.59 ± 0.36
Paraffin	0.794	0.825	0.793	12.26 ± 0.15	13.69 ± 0.14	12.70 ± 0.36
Lubricant 1	0.835	0.891	0.886	14.22 ± 0.17	14.03 ± 0.12	13.90 ± 0.38
Lubricant 2	0.855	0.914	0.875	12.78 ± 0.15	13.93 ± 0.14	12.10 ± 0.36

Ref 1 Jonah *et al*, 1999

Ref 2 Akaho *et al*, 2001

The general trend of the results seems to be in agreement with similar studies carried out in Ghana by Akaho *et al* [2001] and in Nigeria by Jonah *et al* [1999]. However, there are slight deviations which may be attributed to differences in sources and levels of refinements of the products. For example, while Akaho *et al* [2001] and this work reported less hydrogen concentration in petrol compared to kerosene, the reverse is reported by Jonah *et al* [1999]. Also there is a slight disagreement between the present work and Akaho *et al* [2001] on whether the hydrogen concentration is less or greater in diesel compared to petrol.

From the results, it could be stated that the set-up can now be used for quality control of crude oil, refined petroleum products as well as oils for household uses such cooking and cosmetics, by using the appropriate standard products for calibration as demonstrated in this work.

Chapter Six

Conclusions and Recommendations

6.0 Introduction

This chapter presents the outcome of this study and some recommendations for further studies.

6.1 Conclusions

The neutron irradiation facility has a great potential for use in elemental analysis. In particular, the source could be used for determination of low atomic mass elements for which the XRF method is unsuitable.

The following are the specific conclusion arrived at:

- The characterization of the irradiator revealed that optimum thermal neutron activation analysis of samples could be performed at 1.5 – 3.0 cm distance from the source. However, large volumes of samples can be analyzed by taking advantage of a fairly constant optimal flux distribution from 0.0 - 6.0 cm. Fast neutron activation can also be done at any point but preferably as close as possible to the source. When there is concern over possible interferences between reactions caused by thermal and those caused by fast neutrons, the optimization

of irradiation positions should be carried out by comparing the curves of thermal and fast neutrons fluxes distributions. The characterized facility was used for the determination of hydrogen content in petroleum products demonstrating an important application for the facility in quality control of oil-based products.

- The facility has also been used to determine Si and Al content in pulverized geological/ archaeological materials. A method for discriminating the interferences arising in determining Al in the presence of Si was also developed.

6.2 Recommendations

The following recommendations are made with a view of improving the performance of the irradiation facility.

- In the case of hydrogen content determination, large surface area thermal neutron probes (In foil) should be applied. This will ensure that most of the reflected thermal neutrons from the sample are recorded. Another improvement that will see increased efficiency is reduction of the cooling time, for example by bringing both the irradiation and counting facilities under the same roof. In the course of this study, the HPGe detector and the associated electronics developed problems which caused drifting in the gamma spectra and

caused the work to be suspended on many occasions. In order to maximize the applicability of this facility it will be prudent to solve this problem either by repairing the system or replacing the damaged components.

- Apart from the above recommendation, further improvement in the determination of Al and Si could be achieved via increasing the sample weights.
- There is need for the irradiation facility's geometry to be reconstructed to optimize the irradiation potentials of the source. The new geometry should provide channels, i.e. more access to the source from different directions, in order to maximize on its application. The channels could be of different dimensions to cater for different samples sizes and types, including calibration of neutron dosimetric devices.
- Necessary radiation protection measures should also be put in place to ensure the safety of the users and other people who may come close to the facility. Specifically personal monitoring and area monitoring devices, such as TLD and electronic dosimeters should be acquired and used appropriately.
- Create awareness by providing more information about the availability and usefulness of the source. Organize trainings, workshops etc and encourage more students to carry out

research using the source. Also organize training programs in collaboration with the other established research centres and international organizations such as IAEA and many others, so that students and lecturers may visit and learn more about the applications of the isotopic neutron source.

References

Akaho, E. H. K., Jonah, S. A., Dagadu, C. P. K., Maakuu, B. T., Anim-Sampong, S., Kyere, A. W. K., [2001]. Thermal neutron reflection method for measurement of total hydrogen contents in Ghanaian petroleum products. **Appl. Radiat. Iso.** 55, 617-622.

Akaho, E. H. K., Jonah, S. A., Nyarko, B. J. B., Osae, S., Maakuu, B. T., Serfor-Armah, Y., Kyere, A. W. K., [2002]. Simultaneous use of neutron transmission and reflection techniques for the classification of crude oil samples. **Appl. Radiat. Iso.** 57, 831-836.

Amaldi, E., and Fermi, E., [1936]. On the absorption and diffusion of slow neutrons. **Phys. Rev.** 50, 899-928.

Ambrosi, R. M., Talboys, D. L., Sims, M. R., Bannister, N. P., Makarewicz, M., Stevenson, T., Hutchinson, I. B., Watterson, J. I., Lanza, R. C., Ritcher, L., Mills, A., Fraser, G. W., [2005]. Neutron activation analysis, gamma ray spectrometry and radiation environment monitoring instrument concept: GEORAD. **Nucl. Instr. and Meth. A** 539, 198-216.

Borsaru, M. and Eisler, L. P., [1981]. Simultaneous determination of silica and alumina in bulk bauxite samples by fast neutron activation. **Anal. Chem** 53 (12), 1751-1754.

Braun, D., [2006]. Elemental determination of Si and Al concentration in geological/ archaeological samples (in private communication).

Cember, H., [1985]. **Introduction to Health Physics**. Pergamon Press. Oxford

Currie, L. A., [1968]. Limit for qualitative detection and quantitative determination. Application to Radiochemistry. **Anal. Chem.** 40 (3), 590.

Das, H. A., Faanhof, A., Van Der Sloot, H. A., [1989]. **Radioanalysis in Geochemistry**. Elsevier Science publishers BV, 175-186.

Dostal, J., Elson, C., [1980]. Short course in NAA in the Geosciences. In G. K. Muecke (Editor). **General Principles of NAA,** Mineralogical Association of Canada, 28.

Dybczyński, R.S., [2004]. The position of NAA among the methods of inorganic trace analysis in the past and now. **Proceeding of the enlargement workshop on Neutron Measurements, Evaluations and Application (NEMEA),** Bucharest, Romania, 20 – 23 October, 2004, 85-87.

Garg and Batra, [1986]. Isotopic sources in neutron activation analysis. **J. Radioanal. Nucl. Chem.,** 98, 167-198.

Glascock, M. D. and Neff, H., [2003]. Neutron activation analysis and provenance research in archaeology, **Meas. Sci. Technol.** 14, 1516-1526.

Glascock, M. D., Neff, H., Vaughn, K. J., [2004]. INAA and multivariate statistics for Pottery provenance. **Hyperfine Interactions** 154, 95-105.

Glasstone, S. and Sesonke, A., [1994]. **Nuclear Reactor Engineering Reactor Design Basics** 4th Edition, 1.

Gubbi, G. K., [2004]. Neutron detectors. In: G. A., Rama Rao (Editor). **International Association of Nuclear Chemists and Allied Scientists Bulletin**, 247.

Hertzog, R. C., Soran, P. D., Schweitzer, J. S., [1985]. In V. Piksaikin and A. Lorenz (Editors) Subsurface Geochemistry: II. Detection of Na, Mg, Al, and Si in wells with reaction generated by 14MeV neutrons. **Nuclear Data for applied Nuclear Geophysics.** International Nuclear Data Committee (INDC) – 184, 119-130.

IAEA, [1988]. International Atomic Energy Agency. **Isotopic Neutron Sources for NAA, User's Manual** Technical Document No.465. IAEA, Vienna.

IAEA, [1993]. International Atomic Energy Agency. **Handbook on Nuclear Data for Borehole Logging and Mineral Analysis,** Technical Report No. 357. IAEA, Vienna.

IAEA, [1999]. International Atomic Energy Agency. **Nuclear Geophysics and its application** Technical Report No. 393. IAEA, Vienna.

Idris, Y., Funtua, I. I., Umar, I. M., Elegba, S. B., [1998]. Neutron activation analysis of aluminium with Am-Be neutron source-

application for bauxite investigation in Nigeria. **Appl. Radiat. Iso.** 49(1-2), 41-42.

Jonah, S. A., El-Megrab, A. M., Varadi, M., Csikai, J., [1997]. A improved neutron reflection setup for the determination of H and (O + C)/H in oil samples. **J. Radioanal. Nucl. Chem.** 281 (2), 193-195.

Jonah, S.A., Zakari, S. B., and Elegba, S.B., [1999]. Determination of total hydrogen content in oil samples in Nigeria using an Am-Be. **Appl. Radiat. Iso.** 50, 981-983.

Jonah, S. A., Oladipo, M. O. A., Umar, I. M., Rabiu, N., Idris, U. Y., Zakari, Y. I., [2004]. A quick method for the determination of Al/Si weight ratio in alumino-silicates using an Am-Be neutron source. **J. Radioanal. Nucl. Chem.**, 262 (2), 501-504.

Kasztovszky, Z., [2004]. Non-destructive analysis of historical silver coins. **Analytical applications of Nuclear Techniques.** IAEA Vienna, 177-180.

Koch, R. C., [1960]. **Activation Analysis Handbook**. Academic Press New York.

Knoll, G. F., [1979]. **Radiation detection and measurement**. John Wiley & Sons, Inc. Eds.

Knoll, G. F., [1985]. Radioisotope neutron sources – Characteristics and Applications. **Research Reactors and Alternative devices for research**. IAEA-Technical Document No. 351, 21-37.

Krane, K., [1988]. **Introductory Nuclear Physics**. John Wiley& Sons, Inc., Toronto, Canada.

Kreft, A., Bolewski J. R. and Ciechanowski, M., [1989]. An Isotopic neutron source method for measuring the thermal neutron absorption cross section of rocks using small samples. **Nucl. Geophys.** 3(4), 367-372.

Leach, F., [1997]. New Zealand and Oceanic obsidians: an archaeological perspective using neutron activation analysis. **J. Royal Society of New Zealand**. 26, 79-105.

Mohapatra, D. K., Reddy, C. P., [2001]. Use of neutron reflection method to assay nuclear materials in solutions. **Appl. Radiat. Iso.** 55, 693-696.

Moses, J.A., [1964]. **Nuclear techniques in Analytical Chemistry**, Permagon Press Ltd.

Munita, C. S., [2004]. Neutron activation analysis applied to archaeological problems. **Analytical applications of Nuclear Techniques**. IAEA Vienna, 165-170.

Mustapha, A. O., [1992]. Characterization of the moderated neutron field around an Isotopic ^{241}Am-Be source. **MSc. Thesis**. Ahmadu Bello University.

Nunes, J.C., Cross, W.G., and Waker, J. A., [1997]. Feasibility of creating 'CANDU® - LIKE' workplace Neutron fields in an existing irradiation facility. **Rad. Prot. Dosim.** 72 (1), 11-20.

Rapisarda, M., Samuelli, M., [1999]. A portable neutron source for Landmine detection. **Intern. Conf. on Application of Nuclear Techniques "Nuclear Technology for Safety, Security and Industrial Development" Crete, Greece** June 20-26, 1999.

Schweitzer, J. S., Hertzog, R. C., Soran, P. D., [1985]. In V. Piksaikin and A. Lorenz (Editors) Subsurface Geochemistry: II. Nuclear data for Spectroscopic analysis. **Nuclear Data for applied Nuclear Geophysics**, International Nuclear Data Committee (INDC) – 184, 47-61.

Soete, D., Gijbels, R. and Hoste, J., [1972]. **Neutron Activation Analysis.** Wiley-Interscience, New York.

Sudarshan, K., Acharya, R. N., Nair, A. G., Sundia, Y. M., Goswami, A., Reddy, A. V., Manohar, S. B., [2001]. Determination of Prompt K_0 factors in PGNAA. **Development of Prompt γ- ray NAA,** INDC (NDS)-424, 39-43.

Trainer, M., [2002]. Neutron activation: an invaluable technique for teaching applied radiation. **European J. of Physics** 23, 55-60.

Tykot, R. H., [2004]. Scientific methods and applications to archaeological provenance studies. In M. Martini, M. Milazzo and M. Piacentini (Editors) **Proc. of the Intern. School of Physics "Enrico Fermi" Course CLIV**, IOS Press, Amsterdam, 407-437.

United States Geological Survey (USGS), [2007]. Certificates of analysis of geological standards (www.usgs.gov).

Win, D. T., [2004a]. Neutron Activation Analysis. **AU J.T.**, 8 (1), 8-14.

Win, D. T., [2004b]. A Critique on Thermal NAA Estimation of Coinage Metals in Ancient Myanmar Coins. **AU J.T.**, 8 (2), 55-61.

Zamboni, C. B., Zahn, G. S., Shtejer-Diaz, K., Filho, T.M., De Lima, R. B., [2001-2002]. Neutron flux distribution in an Am-Be neutron irradiator. In: A. W. Carbonari (Editor) **Research Reactor Centre – CRPq Progress Report**, 34.

Zevallos-Chávez, J. Y. and Zamboni, C. B., [2005]. Evaluation of the Neutron Flux Distribution in an Am-Be Irradiator using the MCNP-4C Code. **Brazilian Journal of Physics**, 35(3B), 797-800.

Appendix 1

Samples of Gamma-ray spectra of samples before and after irradiation

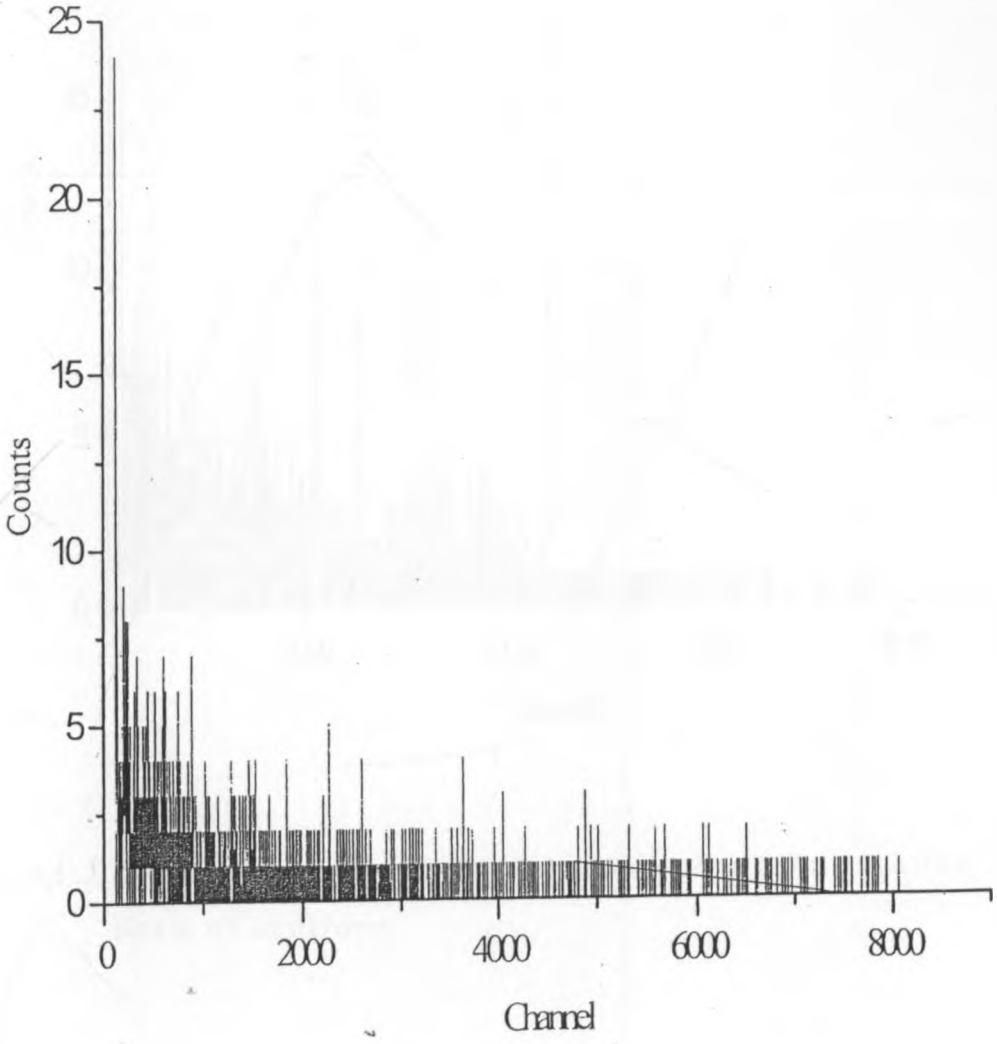

Fig. A1.1 Background of RGM-1 standard before activation in a beam of neutrons.

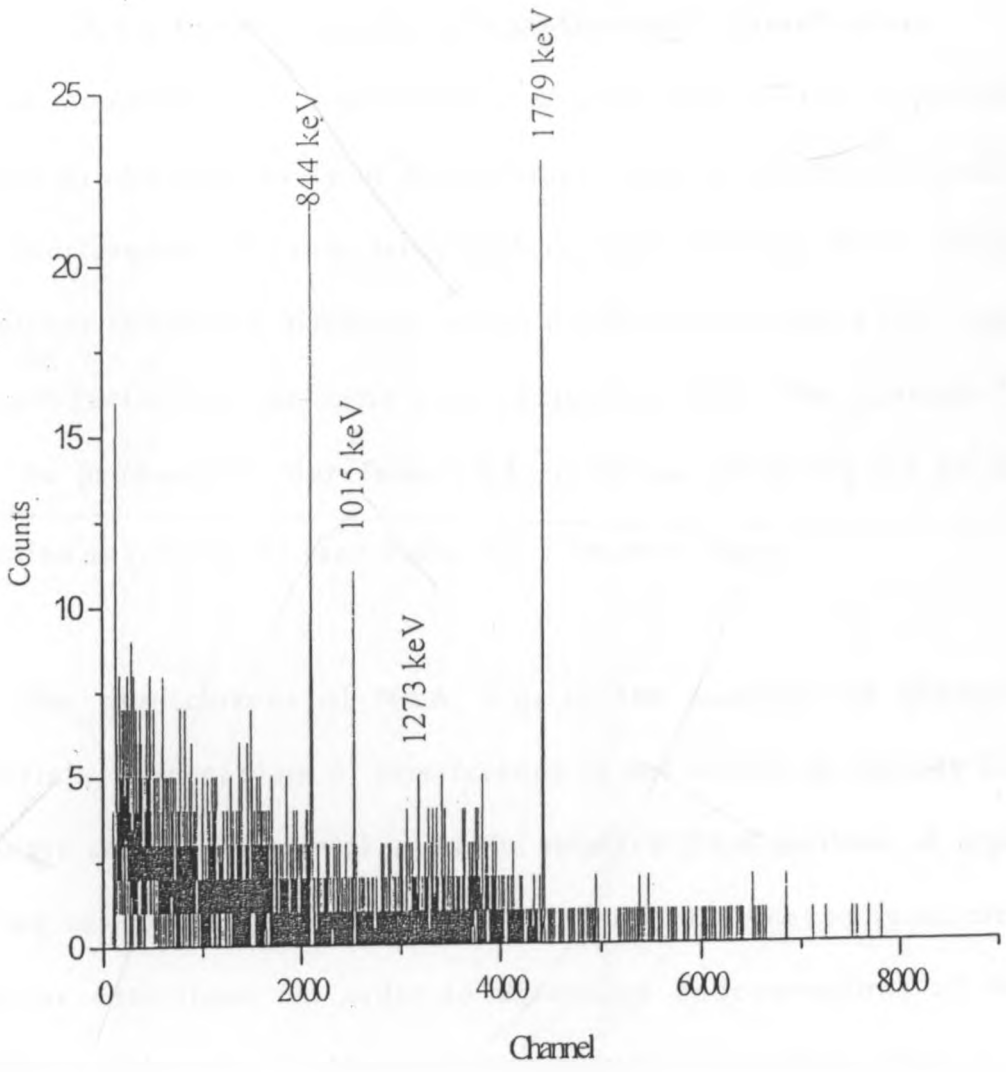

Fig. A1.2 Gamma spectrum of RGM-1 standard after activation in a beam of neutrons.

Appendix 2

NAA in the presence of spectroscopic Interference

In an inhomogeneous and complex neutron flux as that experienced in the irradiation cavity of an howitzer, there is always the problem of interference. This is attributed to contributions from different reactions involving different parent nuclei and neutrons that lead to the production of the same excited nuclear state. For example ^{28}Al can be produced either from (n,γ) reaction involving Al or (n,p) reaction involving Si (see Table A2.1 on next page).

In some applications of NAA, e.g. in the analyses of geological materials, the problem of interference is not solved by merely using a single standard material as in the relative NAA method. A typical geological material contains many elements that cause interference in their detections. In order to determine concentrations of these elements (like Al, Si, Mg etc) in geological materials there is the need to develop a method that eliminates the interferences. Such a method was described by Hertzog *et al* [1985] and is now adapted in this study. The method involves the use of suitable standards containing the elements of interest to estimate the necessary corrections. The ^{29}Si (n,p) ^{29}Al reaction is free of interference [Koch, 1960]. Thus the 1273 keV gamma line produced following

the decay of ^{29}Al nuclide can be used to determine the Si concentration accurately.

Table A2.1 Reactions involved in the detection of Na, Mg, Al and Si from the delayed activity [Adapted from Hertzog *et al*, 1985].

Initial isotope	Reaction	Delayed gamma-ray energies (keV)	Half-life
^{23}Na	(n,γ)	^{24}Na (2754, 1368)	15 hrs
^{23}Na	(n,α)	^{20}F (1633)	11 secs
^{24}Mg	(n,p)	^{24}Na (2754, 1368)	15 hrs
^{26}Mg	(n,γ)	^{27}Mg (844, 1014)	9.45 mins
^{27}Al	(n,α)	^{24}Na (2754, 1368)	15 hrs
^{27}Al	(n,p)	^{27}Mg (844, 1014)	9.45 mins
^{27}Al	(n,γ)	^{28}Al (1779)	2.25 mins
^{28}Si	(n,p)	^{28}Al (1779)	2.25 mins
^{29}Si	(n,p)	^{29}Al (1273)	6.52 mins
^{30}Si	(n,α)	^{27}Mg (844, 1014)	9.45 mins
^{31}P	(n,α)	^{28}Al (1779)	2.25 mins

The yield or time corrected count rate (Y_{Si}) of ^{29}Al induced in a sample can be defined in terms of the Si concentration in the irradiated sample as:

$$Y_{Si} = R_{29n,p}\,\omega_{Si} \qquad \text{A2.1}$$

where

ω_{Si} - is the concentration of Si (%)

Y_{Si} - time corrected count rate (cps)

$R_{29n,p}$ is the reaction rate of the $^{29}Si\ (n,p)\ ^{29}Al$ reaction and is given by Hertzog *et al* [1985]:

$$R_{29n,p} = \int_{v}\int_{E}\sigma(E)\phi(r,E)dE\,dv \quad \text{.....A2.2}$$

where

$\sigma(E)$ - energy dependent cross section (barns)

$\phi(r,E)$ - position and energy dependent neutron flux ($ncm^{-2}s^{-1}$)

v - Volume element

The reaction rates are energy dependent products of reaction cross sections and neutron fluxes and they also depend on position (r), i.e. on the irradiation and counting geometries. Therefore one can determine the reaction rate corresponding to a specific experimental set-up comprising reproducible irradiation as well as counting geometries. To determine R_{29np}, a geological standard which has known Si concentration (ω_{Si}) was irradiated, the value of Y_{Si} under 1273 keV line of ^{29}Al was evaluated and the reaction rate value was computed using equ. A2.1

To determine Al through $^{27}Al\ (n,\gamma)\ ^{28}Al$ in a sample that contains Si, there is need to make corrections due to contribution from $^{28}Si\ (n,p)\ ^{28}Al$ reaction. There may also be contributions from $^{31}P\ (n,\alpha)\ ^{28}Al$ reaction, except where the ratio of P/Si is low as in some geological materials [Hertzog *et al*, 1985]. Assuming negligible contribution from the $^{31}P\ (n,\alpha)\ ^{28}Al$ reaction then;

Al conc. (corrected) = Al conc. (uncorrected) – correction due to Si conc.

i.e.

$$\omega_{Al} = \frac{Y_{Al}}{R_{27n,\gamma}} - \frac{Y_{Si}}{R_{29n,p}} * \frac{R_{28n,p}}{R_{27n,\gamma}} \quad \text{.....A2.3}$$

where

conc. - concentration

ω_{Al} - the Al concentration (%)

Y_{Al} - time corrected count rate of 1779 keV line (cps)

Y_{Si} - time corrected count rate of 1273 keV line (cps)

$R_{28n,p}$ *and* $R_{27n,\gamma}$ - are also the reaction rates for the $^{28}Si\ (n,p)\ ^{28}Al$ and $^{27}Al\ (n,\gamma)\ ^{28}Al$ reactions.

Since the concentration of Si is known from equation A2.1, the above equation may further be expressed as:

$$\omega_{Al} = \left[Y_{Al} - \omega_{Si} R_{28n,p}\right] \frac{1}{R_{27n,\gamma}} \quad \text{A2.4}$$

Detection Limit

Using the developed priori detection limit equation [adapted from Currie, 1968]

$$L_D = 2.71 + 4.65\sqrt{N_B} \quad \text{A2.5}$$

where

L_D is the detection limit (counts) and N_B is the background count.

Upon comparing equation A2.5 with the one used to determine the concentration (equation A2.1). The above equation may be rewritten in terms of concentration. Such that

$$L_D(\omega) = \frac{1}{R}\left[\frac{2.71}{T_c} + 4.65\sqrt{\frac{Y_B}{T_C}}\right] \quad \text{A2.6}$$

where R is the reaction rate, T_C is the counting time after irradiation procedure, Y_B is the background yield (counted before irradiation).

In the case Y_B is zero, which was the case in this study due to the limitation of short T_i and half-lives of the product radionuclides, equation reduces into:

$$L_D = \frac{1}{R}\left[\frac{2.71}{T_c}\right] \quad \text{.....A2.7}$$

Hence the detection limit for Silicon and Aluminium in absence of interference using this procedure is

$$L_D(Si) = \frac{1}{R_{29\,n,p}}\left[\frac{2.71}{T_c}\right] \quad \text{.....A2.8}$$

and

$$L_D(Al) = \frac{1}{R_{27\,n,\gamma}}\left[\frac{2.71}{T_c}\right] \quad \text{.....A2.9}$$

Appendix 3

Certificate of Analyses for the reference standards (Adapted from [USGS, 2007]

PRELIMINARY

USGS ***United States Geological Survey***
Certificate of Analysis

Granodiorite, Silver Plume, Colorado, GSP-2

Material used in the preparation of GSP-2 was collected by the U.S. Geological Survey, from the Silver Plume Quarry, which is located approximately 800 meters west of Silver Plume, Colorado. This is same location used to provide material for GSP-1. GSP-2 is a medium grained hypidiomophic-granular rock consisting essentially of quartz , plagioclase, microcline, biotite, and muscovite. Details of the collection, preparation, and testing are available (Wilson, S.A., 1998).

Element concentrations were determined in a round robin study involving 20 international laboratories. Recommended values are listed when analytical results provided by three independent laboratories using a mininmm of three independent analytical procedures are in statistical agreement. Information values with standard deviations are listed when at least four independent laboratories using two independent analytical procedures have provided information. Information values without standard deviations represent information from a single laboratory or analytical procedure.

Recommended values

Element	Wt %	±	Oxide	Wt %	±
Al	7.88	0.11	Al_2O_3	14.9	0.2
Ca	1.50	0.04	CaO	2.10	0.06
Fe_{tot}	3.43	0.11	$Fe_2O_{3\,tot}$	4.90	0.16
K	4.48	0.12	K_2O	5.38	0.14
Mg	0.58	0.02	MgO	0.96	0.03
Na	2.06	0.07	Na_2O	2.78	0.09
P	0.13	0.01	P_2O_5	0.29	0.02
Si	31.1	0.4	SiO_2	66.6	0.8
Ti	0.40	0.01	TiO_2	0.66	0.02

Element	µg/g	±	Element	µg/g	±
Ba	1340	44	Pb	42	3
Ce	410	30	Rb	245	7
Co	7.3	0.8	Sc	6.3	0.7
Cr	20	6	Sm	27	1
Cu	43	4	Sr	240	10
Eu	2.3	0.1	Th	105	8
Ga	22	2	U	2.40	0.19
La	180	12	V	52	4
Mn	320	20	Y	28	2
Nb	27	2	Yb	1.6	0.2
Nd	200	12	Zn	120	10
Ni	17	2	Zr	550	30

Information values

Element	µg/g	±	Element	µg/g	±
Be	1.5	0.2	Ho	1.0	0.1
Cs	1.2	0.1	Li	36	1
Dy	6.1		Lu	0.23	0.03
Er	2.2		Mo	2.1	0.6
F	3000		Pr	51	5
Gd	12	2	Tl	1.1	
Hf	14	1	Tm	0.29	0.02

Bibliography

Wilson, S.A., 1998, Data compilation for USGS reference material GSP-2, Granodiorite, Silver Plume, Colorado, U.S. Geological Survey Open-File Report (in progress).

Glossary

Wt %	Weight percent of element/oxide as received
µg/g	Micrograms of element per gram of sample, as received
±-	One standard deviation

Denver, Colorado Dr. Linda Gunderson
November 1998

U.S. Geological Survey
Central Region Mineral Team

Ordering Information

USGS reference materials (RMs) may be obtained directly from Dr. Stephen A. Wilson at the address or numbers listed below. The price for each bottle of RM is $65.00 (U.S.) **except** DGPM-1 which is $150.00 (U.S.). This cost includes all shipping and handling charges using normal mail delivery. Urgent requests for RMs should be initiated by FAX or e-mail. If required, overnight delivery is available with these charges added to the final bill.

Dr. Stephen A. Wilson
U.S. Geological Survey
Box 25046, MS 973
Denver, CO 80225

Tel: 303-236-2454
FAX: 303-236-3200 or 303-236-1425
e-mail: swilson@usgs.gov

Payment Procedure

Domestic customers: Payment options include purchase order, check, money order, or credit card (Visa, Mastercard).

International customers: Payment on foreign orders may be made by any of the following:

a. Banker's draft against U.S.A. bank,
b. International money order.

PRELIMINARY

USGS *United States Geological Survey*

Certificate of Analysis

Andesite, AGV-2

Material used in the preparation of AGV-2 was collected from the eastern side of Guano Valley, in Lake County, Oregon. This is the same location used to provide material for AGV-1. Information on the mineralogy and classification of AGV-2 is unavailable but it is assumed to be very similar to AGV-1 (Flanagan, 1967, 1969). Element concentrations for AGV-2 were obtained through a round-robin study involving 23 international laboratories.

Element concentrations are recommended if results from three or more independent laboratories using three or more independent analytical procedures are in statistical agreement. Information values with standard deviations are reported when three or more independent laboratories using at least two independent analytical procedures have provided information. Information values without standard deviations represent information from a single laboratory or analytical procedure. All isotopic information is from a single laboratory.

Recommended values

Oxide	Wt %	±	Oxide	Wt %	±
Al	8.95	0.11	Al_2O_3	16.91	0.21
Ca	3.72	0.09	CaO	5.20	0.13
Fe	4.68	0.09	Fe_2O_3T	6.69	0.13
K	2.39	0.09	K_2O	2.88	0.11
Mg	1.08	0.02	MgO	1.79	0.03
Na	3.11	0.09	Na_2O	4.19	0.13
P	0.21	0.01	P_2O_5	0.48	0.02
Si	27.7	0.35	SiO_2	59.3	0.7
Ti	0.63	0.13	TiO_2	1.05	0.22

Element	µg/g	±	Element	µg/g	±
Ba	1140	32	Pb	13	1
Be	2.3	0.4	Pr	8.3	0.6
Ce	68	3	Rb	68.6	2.3
Co	16	1	Sc	13	1
Cr	17	2	Sr	658	17
Cu	53	4	Th	6.1	0.6
Dy	3.6	0.2	U	1.88	0.16
Ga	20	1	V	120	5
La	38	1	Y	20	1
Mn	770	20	Yb	1.6	0.2
Nb	15	1	Zn	86	8
Nd	30	2	Zr	230	4
Ni	19	3			

Information values

Element	µg/g	±	Element	µg/g	±
Cs	1.16	0.08	Lu	0.25	0.01
Er	1.79	0.11	Sb	0.6	
Eu	1.54	0.10	Sm	5.7	0.3
F	440		Sn	2.3	0.4
Gd	4.69	0.26	Ta	0.89	0.08
Hf	5.08	0.20	Tb	0.64	0.04
Ho	0.71	0.08	Tl	0.27	
Li	11		Tm	0.26	0.02

Element	Ratios	±	N
$Pb^{206}/_{204}$	18.864	0.007	1
$Pb^{207}/_{204}$	15.609	0.006	1
$Pb^{208}/_{204}$	38.511	0.020	1

Bibliography

Wilson, S.A., 1998, Data compilation and statistical analysis of intralaboratory results for AGV-2, U.S. Geological Survey Open-File Report (in progress).

Glossary

Wt %	Percent of total element concentration
µg/g	Total element concentration expressed as micrograms of element per gram of solid sample
±	One standard deviation
N	Number of labs reporting

Issued 4-30-98
Denver, Colorado

Dr. Geoff Phmlee
U.S. Geological Survey
Central Region Mineral Team

Ordering Information

USGS reference materials (RMs) may be obtained directly from Dr. Stephen A. Wilson at the address or numbers listed below. The price for each bottle of RM is $65.00 (U.S.) except DGPM-1 which is $150.00 (U.S.). This cost includes all shipping and handling charges using normal mail delivery. Urgent requests for RMs should be initiated by FAX or e-mail. If required, overnight delivery is available with these charges added to the final bill.

Dr. Stephen A. Wilson
U.S. Geological Survey
Box 25046, MS 973
Denver, CO 80225

Tel: 303-236-2454
FAX: 303-236-3200 or 303-236-1425
e-mail: swilson@usgs.gov

USGS *United States Geological Survey*
Certificate of Analysis

Rhyolite, Glass Mountain, RGM-1

The rhyolite, from Glass Mountain, Siskiyou County, California, was collected from a single block of massive obsidian near the terminal front of a Holocene obsidian flow. The sample is classified as a rhyolite on the basis of its high silica and total alkali contents, and it is assigned to the calc-alkali series because of its high CaO to total iron ratio.

The concentrations were determined by cooperating laboratories using a variety of analytical methods. Values reported are derived from international data compilations (Abbey, 1983, Gladney and Roelandts, 1988, Govindaraju, 1994). Initial USGS reports (Flanagan, 1976) provide background information on this material.

Recommended values

Oxide	Wt %	±	Oxide	Wt %	±
SiO_2	73.4	0.53	MnO	0.036	0.004
Al_2O_3	13.7	0.19	Na_2O	4.07	0.15
Fe_2O_3	0.50	0.01	K_2O	4.30	0.10
FeO	1.27	0.05	TiO_2	0.27	0.02
Fe_2O_3T	1.86	0.03	CaO	1.15	0.07
			MgO	0.28	0.03

Element	µg/g	±	Element	µg/g	±	Element	µg/g	±
Ag	0.11	0.008	Eu	0.66	0.08	Sb	1.3	0.1
As	3.0	0.4	F	340	30	Sc	4.4	0.3
B	28	3	Ga	15	2	Sm	4.3	0.3
Ba	810	46	Gd	3.7	0.4	Sn	4.1	0.4
Be	2.4	0.2	La	24	1.1	Sr	110	10
Br	1.3	0.1	Li	57	8	Ta	0.95	0.1
Ce	47	4	Lu	0.4	0.03	Th	15	1.3
Cl	510	50	Mn	280	30	U	5.8	0.5
Co	2.0	0.2	Mo	2.3	0.5	V	13	2
Cs	9.6	0.6	Nb	8.9	0.6	W	1.5	0.18
Cu	12	1.4	Nd	19	1	Yb	2.6	0.3
Dy	4.1	0.1	Pb	24	3	Zr	220	20
			Rb	150	8			

Element	µg/g	Element	µg/g	Element	µg/g
Cr	3.7	Y	25	Zn	32

Denver, Colorado
revised March 1995

David B. Smith
Branch of Geochemistry

Bibliography

Abbey, S., 1983, Studies in "Standard Samples" of Silicate Rocks and Minerals 1969-1982, Canadian Geological Survey paper 83-15, p-114.

Flanagan, F.J., 1976, Descriptions and Analyses of Eight New USGS Rock Standards, U.S. Geological Survey Professional Paper 840, p 192

Gladney, E.S., and Roelandts, I., 1988, 1987 Compilation of Elemental Concentration Data for USGS BHVO-1, MAG-1, QLO-1, RGM-1, SCo-1, SDC-1, SGR-1, and STM-1, Geostandards Newsletter, 12: 253-362.

Govindaraju, K., 1994, 1994 Compilation of Working Values and Descriptions for 383 Geostandards, Geostandards Newsletter, 18:1-158

Glossary

Fe_2O_3T	Total iron expressed as Fe_2O_3
C_{tot}	Total concentration of carbon
S_{tot}	Total concentration of sulfur
Wt %	Percent of total element concentration
µg/g	Total element concentration expressed as micrograms of element per gram of solid sample
±	One standard deviation

Notes

Unless otherwise indicated total element concentrations are reported for material on an as-received basis, i.e., no drying.

Ordering Information

USGS reference materials (RMs) may be obtained directly from Dr. Stephen A. Wilson at the address or numbers listed below. The price for each bottle of RM is $65.00 (U.S.) **except** DGPM-1 which is $150.00 (U.S.). This cost includes all shipping and handling charges using normal mail delivery. Urgent requests for RMs should be initiated by FAX or e-mail. If required, overnight delivery is available with these charges added to the final bill.

Dr. Stephen A. Wilson
U.S. Geological Survey
Box 25046, MS 973
Denver, CO 80225

Tel: 303-236-2454
FAX: 303-236-3200 or 303-236-1425
e-mail: swilson@usgs.gov

Shipping Date 10-26-79

NUCLEAR SYSTEMS EXPORT, INCORPORATED
924 JOPLIN STREET - P. O. BOX 2543 - BATON ROUGE, LOUISIANA 70821
TEL (504) 383-7791 TELEX 586473

3711

PLEASE REMIT TO ABOVE ADDRESS:

SOLD TO

SHIPPED TO

Invoice Date	
Your Order No.	
Date Shipped	
Shipped Via	
☐ Prepaid ☐ Collect	
TERMS:	

IT\	QUANTITY	DESCRIPTION	UNIT PRICE	AMOUNT
	1 Ea.	301-1[illegible]-0[illegible] 10 Ci. Am 241 Be Neutron Source Model: NB-ED Source Serial No: NB-673 Source Size: 2.2 x 10 MPS Shipped In: NB-20 #0014	4,[illegible]	
2	1 Ea.	301-1060-000 NB-20 Neutron Shipping Device	670.00	670.00
		-7014- Freight Forwarders Charge	42.00	42.00
		TOTAL INVOICE AMOUNT F.O.B. HOUSTON, TEXAS		$5,77[illegible].00

We hereby certify this invoice to be true and correct. We further certify these goods to be products of the United States of America."

"These commodities licensed by the United States for ultimate destination KENYA Diversion contrary to U.S. law prohibited."

Julia Martinez
NUCLEAR SYSTEMS EXPORT, INC.

These goods were produced in compliance with all the requirements of the Fair Labor Standards Act of 1938, as amended.

1-78